UCRL-16314

# University of California

# Ernest O. Lawrence Radiation Laboratory

ORIGIN AND NATURE OF MICROSTRUCTURES

TWO-WEEK LOAN COPY

*This is a Library Circulating Copy which may be borrowed for two weeks. For a personal retention copy, call Tech. Info. Division, Ext. 5545*

Berkeley, California

## DISCLAIMER

This document was prepared as an account of work sponsored by the United States Government. While this document is believed to contain correct information, neither the United States Government nor any agency thereof, nor the Regents of the University of California, nor any of their employees, makes any warranty, express or implied, or assumes any legal responsibility for the accuracy, completeness, or usefulness of any information, apparatus, product, or process disclosed, or represents that its use would not infringe privately owned rights. Reference herein to any specific commercial product, process, or service by its trade name, trademark, manufacturer, or otherwise, does not necessarily constitute or imply its endorsement, recommendation, or favoring by the United States Government or any agency thereof, or the Regents of the University of California. The views and opinions of authors expressed herein do not necessarily state or reflect those of the United States Government or any agency thereof or the Regents of the University of California.

UCRL-16314

UNIVERSITY OF CALIFORNIA

Lawrence Radiation Laboratory
Berkeley, California

AEC Contract W-7405-eng-48

# ORIGIN AND NATURE OF MICROSTRUCTURES

V. F. Zackay and E. R. Parker

September 1965

# ORIGIN AND NATURE OF MICROSTRUCTURES

V. F. Zackay and E. R. Parker

Inorganic Materials Research Division, Lawrence Radiation Laboratory, and
Department of Mineral Technology, College of Engineering,
University of California, Berkeley, California

## INTRODUCTION

The properties of many useful solids (normally polycrystalline and multiphase in nature) can be markedly altered by varying the processes used for shaping the materials and by varying their thermal treatments. For example, a given steel can be made tough and ductile or hard and brittle by simply varying the cooling rate from the "red heat" range. Facts of this kind have been known for many centuries, but it was not until the advent of the optical microscope that the internal changes in structure produced by variations in cooling rate could be distinguished.

During the past half-century, rapid progress has been made in both theory and experiment, and today it is possible for one to actually "see" single atoms in the crystal lattice of a metal. The field ion microscope used for such observations is currently undergoing intensive development and will be an important tool in future studies of the motion and behavior of atoms on an atomic scale. At present, however, our best efforts are confined to the use of transmission electron microscopy for the direct observation of solid state reactions, and the practical limit of resolution of this instrument is of the order of ten atomic spacings. While this instrument has been extremely useful in revealing microstructures much too fine to be observed with a light microscope, there is still a high degree of uncertainty about atomic behavior during solid state precipitation or transformation reactions. Hence many of the concepts about how metastable phases decompose or transform are highly speculative and are subject to change when better research tools become available.

Pure metals are mechanically weak, and to strengthen them, other metals (or elements) are added. Such additions are usually made in the liquid state

where the solubility of foreign atoms is high. In the solid state, however, solubility limits are generally much lower than they are in the liquid, and on cooling the foreign atoms tend to precipitate out of the liquid or solid solutions. When a particle precipitates, it becomes a second phase, homogeneous within itself but separated from the parent material by a well-defined sharp interface. The second phase may be a solid solution consisting mainly of atoms of the added element with some atoms of the parent material intermixed or it may be in the form of an intermetallic compound, i.e., a compound having a stoichiometric composition, such as $Fe_3C$ or $CuAl_2$, but one that does not follow normal chemical valence rules.

Studies of solid state reactions are further complicated by the fact that some pure metals, such as iron and titanium, undergo reactions in the solid state in which, during cooling, the atoms rearrange themselves into a new geometric pattern when a specific temperature is reached. Pure iron in the face centered cubic form at temperatures above 910°C changes to the body centered cubic form when cooled below this temperature. Similarly, the crystal structure of titanium changes from bcc to close-packed hexagonal when cooled to below 880°C. The solubility of foreign atoms is strongly dependent upon the crystal structure. At 720°C, for example, 0.8 weight percent of carbon can be dissolved in the fcc form of iron, whereas only 0.025 percent can be contained in the bcc lattice at the same temperature. Thus phase changes can drastically alter the tendency for a dissolved element to precipitate, and can greatly alter the rate at which a new phase will form and grow. The shape of a newly formed particle is also markedly dependent upon several factors.

So many different transformations can occur in solids that it is necessary to classify them in some orderly manner in order to be able to understand the behavior of solid materials. The word "transformation" is used frequently in discussing solid state reactions to mean "any extensive rearrangements of

the atomic structure," and it is used herein in this sense. Certain reactions require that a nucleus of the new phase must reach a certain critical size before the transformation can proceed. The critical size of a nucleus is dependent upon several factors, and the rate at which it can grow is also dependent upon the conditions existing at the time. Once a stable nucleus has formed, the transformation process continues by "growth". The term "nucleation and growth" is used to describe or define a reaction of this kind. Other types of reactions do not require the formation of a nucleus and the growth processes, which will be described in detail later, are much different in these cases.

The driving force for any transformation is the difference in free energy of the initial and final states and is thus determined by the thermodynamic parameters that apply to large volumes of the phase concerned. Transformations can occur in pure metals as well as in alloys. In a pure metal it is not necessary for atoms to diffuse long distances in order for a phase change to occur (such as the change from fcc iron to bcc iron) upon cooling through the transformation temperature. There are two ways in which the atoms of a pure metal can rearrange themselves with respect to their neighbors to form a new crystal structure from the pre-existing one. One of these is by a nucleation and growth process, which necessarily involves diffusion, and the other is a process that does not involve diffusion--generally called a "martensitic reaction". In the first case, the new phase grows at the expense of the old by relatively slow migration of the phase boundary, and the growth results from atom by atom transfer across this boundary, with the atoms transferring essentially independently of one another. Only short range diffusion along the phase boundary is involved, with many atoms moving less than a single atomic spacing. The new crystals grow into the matrix of the old material, finally

consuming the entire volume of the primary phase. Figure 1 is a photomicrograph showing a nucleation and growth transformation of the so-called "massive" type in which particles of the new phase are large and blocky. This massive-type nucleation and growth transformation frequently occurs at a relatively high temperature during an allotropic transformation in either a pure metal or a solid solution alloy. A solid solution, however, can also transform in several other ways. A second phase, different in composition, can precipitate in the form of equiaxed crystals, as small uniformly dispersed particles, as a grain boundary film, or in the form of parallel plates. Photomicrographs of some of these structures are shown in Fig. 2.

The martensitic transformation is truly diffusionless, even in alloys. The atomic movement involved does not require thermal energy; in this case all atoms move in unison through distances shorter than one atomic spacing. The time required for this kind of transformation to occur is often many orders of magnitude shorter than that needed for a massive transformation; the interface between the new and the old phase moves with near-sonic velocity into the parent phase. Martensite crystals are usually flat plates which tend to be thin at the extremities and to have lenticular shapes. With this transformation there is always a definite relationship between the orientations of the original crystals and those of the new phase. The primary atomic movement is a shear translation, which, on a polished surface, will produce visible upheavels. The martensite reactions can also be identified metallographically; a characteristic microstructure is shown in Fig. 3.

A more rigorous classification of phase transformations and a detailed comparison of the characteristics of nucleation and growth and martensitic reactions due to Christian [1] is given in Appendix A.

Such variations in the structure of phases and distribution of phases in multiphase systems constitute the development of a microstructure. It is obvious, that, for a given chemical composition, literally an infinite number of microstructures are possible. It becomes important to study the factors that control the nature of microstructures because the microstructure strongly affects the properties and behavior of a given material. This chapter will concern itself with an atomic approach to an analysis of the type and nature of phase transformations that can occur in a material and their control by heat treatment. It will not concern itself with problems of solidification leading to grain size and growth control which, of course, are also critical factors in microstructure development but are best understood on the basis of an energy approach.

## PRECIPITATION FROM SUPERSATURATED SOLID SOLUTIONS

Many metals of technological importance have large solubilities for foreign elements at elevated temperatures and only limited solubilities at low temperatures. It is thus possible to completely dissolve a second component at an elevated temperature and then, by quenching from the high temperature, to retain a single phase supersaturated solid solution at the low temperature. This supersaturated material can then be made to decompose by reheating it to an intermediate temperature. This process forms the basis for the age-hardening treatment given to many useful commercial alloys. In this section we shall consider the experimental results and the theoretical reasoning which lead to an understanding of the mechanism of precipitation; namely, continuous, or general, and discontinuous, or cellular. In continuous precipitation the particles are dispersed throughout the volumes of the material, whereas with discontinuous precipitation localized volumes of the material transform completely into the new equilibrium phases while the bulk of the material remains untransformed. Figures 4 and 5 are photomigrographs showing these two kinds of precipitation. As might be expected, the reaction rates in the two cases are markedly different. In continuous precipitation a linear growth-time behavior is observed. The theoretical analyses which explain the two types of behavior is presented in the following section, with nucleation processes being first described.

### Homogeneous Nucleation

The simplest case of nucleation is one in which a single phase changes into another phase of a different crystal structure without undergoing compositional changes. The condition necessary for a nucleation of a $\beta$ phase in a supersaturated $\alpha$ phase is that the free energy change associated with the phase formation must be negative and that it must be sufficient to supply the energy required to create the interface between the phases $\alpha$ and $\beta$.

The change in free energy, upon formation of a particle of the β phase, is given by the following equation:

$$\Delta G = 4/3\ \pi r^3\ \Delta G_v + 4\pi r^2 \gamma \qquad (1)$$

In this equation $\Delta G$ is the free energy change of the reaction. $\Delta G_v$ is the difference in volume free energy for the β and α phases (per unit of volume); γ is the surface energy per unit of area; and r is the radius of the particle. In this simple theory, the particle is assumed to be spherical. A sketch of the $\Delta G$ versus r curve is shown in Fig. 6. The surface energy term is positive, and its effect predominates when the radius is small. When the radius exceeds $r_c$, however, the volume free energy term predominates and growth of the nucleus becomes possible. In order for a stable nucleus to form, the critical activation energy $\Delta G_r$ must be supplied by thermal fluctuations in the lattice. $\Delta G_r$ and $r_c$ are strongly dependent upon temperature. At the equilibrium temperature, $\Delta G$ for the reaction is zero and consequently $\Delta G_r$ and $r_c$ are equal to infinity. Homigeneous nucleation thus becomes impossible at the temperature of equilibrium. Once the nucleus has reached a certain critical size, it can grow by the transfer of atoms of the parent phase across the interface to the new phase. The expression which relates the rate of growth to the temperature is given below:

$$\frac{di}{dt} = s\nu_o \epsilon^{\frac{-\Delta G_a}{kT}} \qquad (2)$$

In this equation, di/dt is the number of atoms crossing the interface per second; s is the number of atoms in the α phase facing the β phase particle;

$\nu_o$ is the frequency factor, which is the number of times per second that an atom might be able to jump across the barrier (about $10^{13}$/sec in solids). $\Delta G_a$ is a new activation energy--the energy that an atom must have in order to cross the interface between the $\alpha$ and $\beta$ phases; k is Boltzman's constant and T is the absolute temperature. When the growth process is sufficiently slow, the number of stable nuclei of a critical size that will form per unit of time is just equal to the number disappearing through growth. Thus the number of nuclei per unit of volume is given by the following equation:

$$N_e = N_v \epsilon^{\frac{-\Delta G_r}{kT}} \tag{3}$$

$N_e$ is the equilibrium number of nuclei per unit of volume; $N_v$ is the total number of atoms per unit of volume, and $\Delta G_r$ is the activation energy required for the formation of a stable nucleus.

The rate of nucleation, I, is given by the product of Eqs. (2) and (3). The resultant is shown as Eq. (4).

$$I = s\nu_o N_v \epsilon^{\frac{-\Delta G_r + \Delta G_a}{kT}} \tag{4}$$

The above treatment was due to Volmer and Webber.[2] It was improved by Becker and Doring[3] and applied to condensed systems by Turnbull and Fisher.[4] In the original treatment, it was assumed that once an $\alpha$ phase atom had crossed the boundary and attached itself to the $\beta$ phase it could not return to the $\alpha$ phase position. While this assumption is reasonable for values of r much larger than $r_c$, it is not at all reasonable when r is

approximately equal to $r_c$. At this value, it is just as probable that a $\beta$ phase atom will cross the phase boundary and join the $\alpha$ phase. Thus, the rate given by Eq. (4) should be divided by two. The assumption that the number of nuclei forming per unit of time equals the number of those disappearing through growth has also been questioned. The calculations made by Becker and Doring and Turnbull and Fisher indicate that the number of nuclei was not the equilibrium number and that the coefficient $s\nu_o N_v$, shown in Eq. (4), should be modified as indicated below:

$$I = s\nu_o N_v \frac{r^2\gamma}{9kT} \epsilon^{\frac{-\Delta G_r + \Delta G_a}{kT}} \qquad (5)$$

Unfortunately, it has not been possible to establish the validity of the coefficient of the exponential term in Eq. (5). Turnbull attempted to evaluate this coefficient for mercury and obtained 42 for its logarithm, whereas the theoretical value should have been 35; the discrepancy between experiment and theory was thus a factor of $10^7$. It must therefore be concluded that the variable controlling the absolute rate of nucleation was not quantitatively understood. However, the temperature variation of the nucleation rate is reasonably well understood. It is well known that the $\Delta G_a$ term (related to surface energy) in Eq. (5) is insensitive to temperature change, whereas decreases rapidly with decreasing temperature. Thus at very large values of supercooling, $\Delta T$ the $\Delta G_r$ term dominates and I varies exponentially with temperature. A curve showing the qualitative variation of I vs $\Delta T$ is presented in Fig. (7). This type of behavior has been commonly observed.

In the case of a material that has been quenched from a high temperature, the nucleation rate may not be constant. Nuclei of various radii exist at each temperature and some of those established at the higher temperature may have had radii equal to or exceeding the critical radius characteristic

of the lower temperature. Thus in the quenched material, some retained nuclei would immediately begin to grow, while others were forming. Because the free energy for nucleus formation is greater at the higher temperature, there would be fewer than the equilibrium number of nuclei at the lower temperature immediately after quenching. As time at the lower temperature increases, the number of critical nuclei per unit of volume will increase toward the equilibrium number at a rate that is governed largely by $\Delta G_a$. It is possible, however, that the number of nuclei will never reach the equilibrium value because nuclei disappear rapidly due to growth, once they reach the critical size. Thus a steady state value of nuclei concentration less than the equilibrium number might be reached.

In analyzing the transient nucleation problem, Turnbull assumed that the number of nuclei per unit of volume increased from its initial value, $N_o$, to its steady state value, $N_s$, according to the exponential law given in Eq. (6).

$$\frac{N_t - N_o}{N_s - N_o} = \epsilon^{-\omega/t} \qquad (6)$$

In this equation, $N_t$ is the number of nuclei at any time t, and  is the time constant for the process. The time constant is related to $\Delta G_a$. If it is large, a long time would be required to reach the equilibrium value, $N_s$. If $N_o$ is very small, then the rate of nucleation per unit of volume is given by Eq. (7).

$$I_t = I_s \, \epsilon^{-\omega/t} \qquad (7)$$

In some cases, $\Delta G_r$ at the higher temperature is not very much larger than $\Delta G_r$ at the lower temperature. Under these circumstances $N_o$ will be very large. In fact it may be so large that the number of nuclei formed after $T_o$ may be negligible. This case is called "athermal nucleation", and it is particularly important in the martensite transformation of steel and in some age-hardening reactions.

The effects of strain energy on nucleation and the more complex case of heterogeneous nucleation are discussed in Appendix B.

Continuous Precipitation

Continuous precipitation may be classified as either general or local. With general precipitation the distribution of the particles of the second phase is uniform throughout the volume, whereas with discontinuous precipitation nuclei form and grow only in localized volumes. Discontinuous precipitation often spreads from grain boundaries into the grains.

In both types of precipitation, a supersaturated $\alpha$-solid solution decomposes into a saturated $\alpha$ phase and a new second phase. It has been found experimentally that with discontinuous precipitation the orientation of the saturated $\alpha$ phase differs from that of the supersaturated $\alpha$ phase into which it is growing. This means, in effect, that the $\alpha$ phase is recrystallizing, thus the reaction is sometimes called a recrystallization reaction, although this name is misleading because it tends to obscure the picture of how the new phases form.

Continuous precipitation usually occurs in solid solutions of low supersaturation or in those in which the strain energy associated with the reaction is large. The driving force for precipitation is small in this case. Homogeneous nucleation within perfect regions of the crystals is unlikely and "continuous" precipitation is confined to dislocation networks and grain boundaries. There is ample experimental verification for this conclusion.

In the precipitation of copper from germanium, it is well established that the copper nucleates on the dislocation lines. This is also true for the precipitation of copper in silicon. In the precipitation of carbides and nitrides in $\alpha$ iron, the particles may be plate shaped or spherical, but the centers of the nuclei have been observed to lie along dislocation lines in the matrix.

In analyses leading to growth rate laws, it is assumed that the growth velocity depends upon the coefficient of lattice diffusion. This assumption has been tested experimentally by measuring the radius of particles as a function of time. The actual growth rates thus measured and those calculated from diffusion data agree within the limits of experimental error, although these limits were rather wide.

It is difficult to obtain verification of nucleation and growth theories because of the fact that the temperature variation of the precipitation rate depends upon the number of nuclei initially present after quenching and upon the nucleation and growth rates at test temperature.

It has been observed experimentally that the precipitation rate at high carbon contents and low temperatures is enormously high. Furthermore, this high rate of precipitation is not associated with any change in the activation energy for the growth of the precipitating particles. Electron microscope studies of high concentration carbon alloys have shown that it is indeed true that the precipitation occurs not only on dislocation networks but also throughout the matrix. Thus it has been shown that the change in kinetics is due to the onset of precipitation at matrix sites. At higher reaction temperatures, the carbides on the dislocation networks grow at the expense of those in the matrix. At lower temperatures, however, the matrix carbides grow to larger sizes than those formed on the dislocation.

The nucleation of precipitates is strongly dependent upon both temperature

and matrix composition as shown by the studies of Keh and Leslie (5) on Fe-C, Fe-N, Fe-Si-C, and Fe-Mn-C alloys. The time required to initiate precipitation at constant aging temperatures for two Fe-3.3 Si - x C alloys is shown in Fig. (8). The apparently minor difference in carbon content in alloys A and B, A having 0.030% C and B having 0.018% C produces major changes both in the kinetics and in the nucleation sites for precipitation. Keh and Leslie also observed that the presence of silicon in Fe-C alloys suppresses precipitation of carbides in the matrix or on dislocations.

The above analyses apply equally as well to dislocation networks and the same considerations are involved. The energy differences, however, of dislocation networks are less than those of grain boundaries. Consequently, dislocation networks will be less effective as nucleation sites than are the corresponding surfaces, edges, or corners, of the grain boundaries.

Continuous precipitation, i.e. the substantially uniform distribution of nuclei forming throughout the volume of crystalline phases, is commonly observed although it is frequently aided by the presence of dislocation networks. Discontinuous precipitation, on the other hand, is the type which begins locally, not uniformly, and extends generally by growth of clusters or cells into untransformed matrix material.

Discontinuous Precipitation

In discontinuous precipitation, a phase transformation nucleates at some position or place such as a grain boundary and the reaction proceeds by the formation of the new phase and a saturated solution from the original supersaturated phase. The precipitation reaction, i.e. the growth of the cell containing the new phase and the saturated alpha phase, spreads inward toward the center of the grains. It was thought for many years that dis-

continuous precipitation must be preceded by a stage of general precipitation or clustering. This view is no longer held in favor because in some alloys such as lead-tin or gold-nickel the whole reaction appears to be discontinuous. The cells of the product phases must frequently form in lamella, the β-precipitate and the saturated α-phase are not related in orientation to the parent supersaturated alpha. As the cells grow, branching of the plates must occur in order for the nearly spherically growing cells to maintain constant interlamellar spacing.

The nucleation of a cell requires the formation of an incoherent boundary between the saturated alpha phase and its supersaturated parent. This can occur easiest at grain boundaries and this is thought to be an important reason why discontinuous precipitation almost invariably starts at such boundaries. A theory of cell nucleation was offered by C. S. Smith(6) in 1953. It is known that diffusion can occur rapidly along an incoherent grain boundary. Consequently, for the beta region to grow into the alpha, it should grow best when it is in contact with an incoherent interface in the alpha phase, as shown in Fig. 9. If a beta particle is nucleated in grain 1 at the boundary between grains 1 and 2 of an alpha phase and grows into grain 2, it is likely that the orientations between the beta phase and the newly=formed saturated alpha phase will be such as to minimize the interfacial energy between these two phases. Also, if the saturated alpha particlehas the same orientation as the supersaturated grain 1, there will not be an interface between them; hence, there will not be a diffusion short circuit available to aid the growth of the beta grains in the cell can grow into grain 2 because there is an incoherent interface developed in this case between the alpha saturated solution and the alpha supersaturated solution of grain 2. Thus the alpha is growing into the adjacent grain in much the same way as the growth of a grain occurs during recrystallization of a cold-worked metal. The orientation of the alpha in

the cell should not be related to the grain into which it is growing but it should be nearly identical with the orientation of the supersaturated alpha on the other side of the boundary. Smith published a polarized light photomicrograph showing the transformation taking place in a zinc-copper alloy containing 2% copper. In the picture, the major phases in the cells could be seen to have an orientation which was very different from that of the grain into which they were growing but which were indistinguishable from the adjacent alpha grain into which the cells did not grow.

Experimental work on the kinetics of decomposition reactions where discontinuous precipitation was occurring support the conclusion that boundary diffusion plays a primary role in such transformations. The main evidence for this comes from transformation studies occurring at low temperatures, such as lead-tin alloys transforming at -78°C, gold-nickel and gold-cobalt alloys transforming at room temperature. In all these cases, the activation energy for volume diffusion would require that the reaction rates would be extremely small at the temperatures at which relatively rapid growth of cellular precipitates occurred.

Formation of Guinier-Preston Zones

In certain alloy systems, changes occur in short periods of time at low temperatures. Such changes often result in marked increases in hardness and strength. The effects are due to a pre-precipitation, a segregation, or clustering of atoms prior to the actual formation of nuclei or precipitates. These clusters are known as Guinier-Preston zones. They are found in alloys where the differences in atomic size between the solute and solvent atoms is small or where the supersaturation is large. In such cases, cluster nucleation is not difficult. Examples of alloy systems in which this type of segregation occurs are cobalt in copper, silver or zinc in aluminum, and copper in aluminum. In the first three, the size differences are small; in

the latter, the size disparity is large. The zones in the latter case form at high degrees of supersaturation. Although the early evidence for Guinier-Preston zones was obtained by x-ray diffraction techniques, the best evidence, and the most direct, for the existence of such zones is provided by transmission electron microscopy.

Guinier-Preston zones are formed by the clustering of groups of like atoms within the matrix of a solid solution. When there is a difference in atom size, certain planes will be preferential sites for clustering in order that the elastic strain energy associated with such clustering be minimized. In the aluminum-copper system, for example, there are the {100} types of planes. There is, in the case of zone formation, perfect coherence between the zone and the matrix. When the size differences are substantial, however, it is possible only for small zones to exist because of the coherence and the large strain energy associated with the clustering of the solute atoms. The linear dimensions of the clustered zone are of the order of 100Å or less. The actual shape of the zones differs in different alloy systems because of the strain energy factor, with, in aluminum-silver, for example, spherical zones forming, and in aluminum-copper, the zones being plate shaped.

In the clustering associated with Guinier-Preston zone formation, atoms of like kind must gather together by what is termed an "up-hill" diffusion process. The "up-hill" diffusion is possible because of the lower free energy of the clustered atoms.

The formation and growth of zones is somewhat complicated, with several stages being involved in certain cases such as the copper-aluminum alloy systems. The plate-shaped zones shown in Fig.10 are called Guinier-Preston 1, or GP 1 zones. They are responsible for the increase in hardness produced by aging at low temperatures as shown in Fig. 11.

The evidence strongly indicates that in the aluminum copper alloys there are at least four distinct stages: GP1$\rightarrow\Theta''\rightarrow\Theta'\rightarrow\Theta$. It is not known

whether these structures form directly from one another or whether they are independently nucleated with one growing at the expense of the other.

When the aging is carried out at 100°C, for example, the hardness curve shows a rise to a second maximum followed by an eventual decrease. X-ray evidence shows that during this period there are changes in the matrix resulting in the formation of a new structure which has been described in the literature as Θ" or GP2 structure. According to Guinier, the Θ" region consists of layers parallel to {100} planes of the matrix. The structure consists of planes of copper atoms, the adjacent planes 1.9Å units away being mixtures of copper and aluminum atoms; the next planes are 2Å away from the mixed-atom planes and they contain only aluminum atoms. Electron diffraction pictures taken from alloys in this state confirm that the Θ" structure can best be regarded as a genuine precipitate rather than a zone.

Aluminum copper alloys hardened at low temperatures by the formation of Θ" zones begin to soften when the Θ' precipitate becomes visible. The Θ' structure is not an equilibrium phase either but is a coherent precipitate which has a fixed orientation relationship with the matrix. Figure 12 is an electron micrograph of a Θ' structure having plates parallel to {100} planes in the matrix. These plates appear as needles of approximately 20Å in thickness and 300Å long.

The composition of Θ' is very near that of the equilibrium final precipitate $CuAl_2$. The Θ' structure is the first precipitate which may be observed under the optical microscope. At high temperatures it forms directly from the matrix as does the precipitate $CuAl_2$. The Θ' precipitate probably has a partially coherent interface.

The Al-Cu system has been studied very extensively and the changes occurring therein are well known. The complexity of behavior exhibited by this system illustrates clearly the complications that can arise in precipitation reactions.

Spinodal Decomposition

In certain alloy systems, i. e. that of gold and platinum (shown in Fig. 13), the uniform series of solid solutions exists at all compositions at high temperatures. However, at lower temperatures a segregation of alloys occurs and a miscibility gap exists in which saturated solid solutions of platinum-rich and gold-rich phases appear. In such systems, the formation of the two new saturated phases from a quenched supersaturated solid solution may occur either by a nucleation and growth process or by a process known as spinodal decomposition. In systems with miscibility gaps, there is only a change in composition during the phase change. The structures of the two resulting phases and of the initial phase are identical. In special cases of this kind, it is possible for the transformation to occur simply by an exchange of atoms in old lattice sites. This is similar to the formation of Guinier-Preston zones discussed in the previous section. When spinodal decomposition occurs, the normal nucleation process is absent. Spinodal separation can occur only in a restricted region of the miscibility gap, e.g. within the region shown by the dashed line in Fig. 13.

The concept of a spinodal type of transformation originated with Gibbs. In his classical treatment of the stability of phases, he considered two types of decomposition. In one, the change was that of a large fluctuation in composition within a very small volume and the other was that of a very small change in composition in a very large volume. When a phase is unstable to small fluctuations over large volumes, then there is no barrier to continuous transformation to the more stable state other than that involved in a diffusion process. Gibbs showed that a necessary condition for stability to such a fluctuation should be that the chemical potential of each component increases with increasing density of that component. This is equivalent to stating that the second derivative of the free energy with respect to composition

must be less than zero. On a binary phase diagram, the boundary of the spinodal region is defined by the loci of points at various temperatures where the second partial of the free energy with respect to composition is equal to zero. Gibbs' original concepts were confined to the consideration of liquid systems. The concepts have extended to solid solutions by a number of investigators. The validity of the concepts for solid solutions has not been definitely established, but it seems virtually certain that many of the considerations apply equally as well to solid systems.

When a random solid solution alloy is quenched into the spinodal region where the second derivative of the free energy with respect to composition is negative, any small fluctuation in composition will tend to increase. The supersaturated solid solution will begin to segregate spontaneously into regions which are richer in each of the two components. The rate at which this occurs is limited only to the rate of diffusion within the solid solution. Spontaneous segregation of this kind requires net atomic movement in a direction opposite to the concentration gradient and, therefore, involves "up-hill" diffusion. Thus the conditions for spontaneous spinodal separation and up-hill diffusion are identical. Borelius[7] was among the first workers to apply the concepts of spinodal segregation, or separation, to the decomposition of supersaturated solutions. His work was generally believed to be of doubtful significance until Cahn[8] and Hillert [9] in 1961 showed that it was necessary to introduce a surface energy term in order to provide a valid analysis. Because spinodal decomposition generally occurs in systems in which the atoms have different sizes when the segregation takes place, stresses are developed which tend to stabilize the original system and prevent the small local fluctuations from propagating. Three factors contribute to the free energy change associated with a spinodal decomposition. One is the normal chemical term associated with the formation of two new phases from the parent material. There is also a term which arises from the

composition gradient which exists during spinodal segregation. The gradient energy is analogous to surface energy in the case of the formation of a nucleus. This term is a positive free energy term. The third factor is a strain energy which arises from the change in lattice parameter associated with the compositional changes. Because the lattice is coherent, or continuous, the individual small volumes of segregated material cannot relax to their normal, or stress free, states. Hence there will be elastic strain energy stored in the system.

A spinodal decomposition process should occur uniformly everywhere within a grain. It is not easy to distinguish this form of decomposition from a homogeneous nucleation process. The main distinguishing characteristic seems to be that with spinodal decomposition the spacing of the segregated regions is substantially more uniform than it would be with homogeneous nucleation, which is a random process. X-ray diffraction patterns taken during alloys undergoing spinodal decomposition exhibit side bands. These side bands do not correspond to the lattice parameters of the equilibrium phases, but are broad diffuse regions between the positions of the x-ray diffraction lines for the supersaturated solid solution and the two equilibrium decomposition phases. X-ray patterns in systems undergoing nucleation and growth exhibit sharp lines of the new phases forming as a consequence of the decomposition of the supersaturated phase. Spinodal transformation differs from nucleation and growth in that there is no clear stage where the new phase has appeared. The composition gradually changes from that of the supersaturated phase over toward that of the equilibrium phases without the formation of interface boundaries between regions of different homogeneous compositions. In a spinodal system, the spinodal reaction is in competition with nucleation and growth reaction, and often the two occur simultaneously.

The decomposition pattern of a spinodal is remarkably uniform as the photomicrograph in Fig. 14 shows. The wavelength, or distance between, segregated regions is of the order of 100 atom spaces, although it is possible to have wavelengths much smaller or much larger.

Superlattice or Ordered Structures

In an ordinary solid solution, the component atoms are randomly mixed. There are many solid solutions, however, in which a random distribution of atoms does not exist, or if it does, it does so only at high temperatures. In these, atoms of one kind seem to segregate more or less completely on one set of atomic positions, leaving atoms of the other kind in the remaining sites. Such a structure is called an ordered structure and the lattice is called a superlattice. In an ordered structure, alternate planes may be rich in one component and the intermediate planes rich in the other. The distance between identical planes may thus be twice as great as the distance between planes in a disordered structure where the atoms are randomly dispersed. Diffraction patterns of an ordered alloy will therefore contain extra reflections or superlattice lines so that they may be distinguished from random solid solutions. Ordered structures form at relatively low temperatures and are generally of compositions having atomic ratios of either 1:1 or 1:3 of the component elements. Above a certain critical temperature the atoms are randomly intermixed, whereas at lower temperatures order begins to be established and the degree of order increases as the temperature drops. The main theoretical features of the order-disorder reactions have been worked out completely and verified experimentally. Cu-Au provides a classic example of an ordered system with order of one kind existing at 50:50 composition and order of another kind being exhibited at 25% Cu. In the ordered structures there is no nucleation or growth nor is there any spinodal reaction that occurs. The atoms must merely rearrange themselves on a very local basis so that they assume alternate and favored positions in the lattice.

The Massive and Martensitic Transformations

The essential features of "nucleation and growth" and "martensitic-type" reactions are described in the Introduction and are contrasted in detail in Appendix A. The "massive" transformation has some characteristics of both these types of reactions and may be viewed as intermediate between the two. As in martensitic reactions, the composition of the parent and product phases are identical, i.e., there is no long-range diffusion. However, since there is neither a crystallographic relationship between the and product phases nor is there evidence of surface upheaval on a polished section, it must be assumed that the growth of the product phase is thermally activated and that the growth rate is interface controlled. The latter two features are, of course, characteristic of nucleation and growth transformations. The product phase is nucleated at grain boundaries and grows by the thermally assisted movement of individual atoms over a small number of interatomic distances, and, in particular, across the interface from the old phase to the new. The microstructure resulting from a massive transformation differs from that of either the nucleation and growth or the martensitic in that it consists of irregular, blocky and rather jagged boundaries of no particular shape. The principal features of a massive transformation are identical to those of a polymorphic transformation - the term "massive" being reserved for the transformation in alloys[1].

The kinetics of both the massive and martensitic reactions are similar, as Owen et al(10) have shown, in that the transformation temperature is independent of cooling rate below a critical cooling rate, as shown in Fig. 15. Thus, as Christian[1] hypothesizes, the type of transformation that an unstable alloy undergoes upon quenching from a high temperature can be dependent on the cooling rate. At low cooling

rates a nucleation and growth type transformation may predominate; at higher cooling rates where long-range diffusion is suppressed, the massive transformation may occur; and, finally at very high cooling rates there is the possibility of a martensitic reaction. However, the latter is possible only if the driving force is great enough to supply the large strain energy needed for the martensitic reaction.

In view of the similar kinetics of the massive and martensitic reactions, it is not surprising, perhaps, that there are alloy systems in which both reactions are found. A classic example is that of the Fe-Ni system in which three types of transformations have been identified, i.e., nucleation and growth, massive, and martensitic. Owen et al[10] have determined the range of compositions over which each transformation occurs as shown in Fig. 16. For alloys containing less than 5 at. % nickel an equiaxed structure (resulting from a nucleation and growth transformation) was stable even at the highest cooling rates employed (8000°C/sec). At higher nickel contents, the nucleation and growth transformation could be retained by high cooling rates, and in alloys containing greater than 10% nickel only the massive transformation was observed. Between 10 and 29% nickel and for cooling rates greater than 5°C/min (the slowest rate employed) a typical massive microstructure was seen. The authors refer to this microstructure as "massive-martensite", since a shape change (characteristic of martensitic reactions) was observed. Finally, a typical acicular martensitic microstructure was seen in alloys containing 30-33% nickel. Micrographs of massive- and acicular-martensite are shown in Figs. 1 and 2 respectively.

A curious feature of the massive transformation in iron alloys is that it is suppressed either by large amounts of substitutional elements or small amounts of interstitial elements, but not by extremely high

rates of cooling. Furthermore, Owen observed that at the highest cooling rate attainable the transformation of pure iron was martensitic while that of the iron alloys remained massive. At present there is no explanation for this behavior.

A comparison of the principal features of the nucleation and growth, massive, and martensitic transformations is given in Table I.

Table 1 - A Comparison of the Nucleation and Growth, Massive, and Martensitic Transformations

| Characteristic | Nucleation & Growth | Massive | Martensitic |
|---|---|---|---|
| Composition change between parent and product phases | Generally | None | None |
| Type of growth | Thermally activated | Thermally activated | Not thermally activated |
| Nature of diffusional process | Long range | Short range (equivalent to grain boundary diffusion) | None |
| Velocity of transformation | Slow | Fast | Fastest (with rare exception) |
| Shape change | None | Occasionally | Always |
| Crystallographic relationship between parent and product phases | Generally none | None | Always |
| Free energy change | None at equilibrium | Small | Large |
| Amount of undercooling | None | Small | Large |
| Nucleation sites | Generally at structural defects | At grain boundaries | Unknown |

# APPENDIX A

## A Classification of Phase Transformations in Metals

Natural phenomena rarely lend themselves to rigorous systems of classification and solid state transformations are no exception. However, Christian [1] in his forthcoming book Theory of Transformations in Metals and Alloys proposes a useful classification which is presented herein in somewhat simplified form. The authors are indebted to Dr. Christian for his permission to use this material.

Solid state transformations can be conveniently divided into two large groups based on the type of nucleation, and then further subdivided in terms of their growth processes. Transformations are considered to proceed either from identifiable nuclei, i.e., heterogeneously, or spontaneously without nucleation, i.e., homogeneously, as shown in the first line of Table 2 under "Type of Nucleation."

The nature of the growth process of heterogeneously nucleated solids forms the basis for the next subdivision in the classification, as shown under "Thermal Characteristics" of the table. Thus, the first type of growth process is "athermal", i.e., the growth is not thermally activated and does not involve diffusion. In this case the boundary of the growing phase is glissile and moves by stress alone. Examples of this type of transformation are martensitic reactions, twinning, and the stress-induced movement of low angle grain boundaries. The second type of growth process involves thermal activation, i.e., either short- or long-range diffusion. The phase boundary interface is non-glissile and the rate of growth is diffusion-limited. Examples of transformations of this type wherein the growth rate is controlled by interface reactions,

Classifications of Transformations*

Table 2

| Type of Nucleation | Heterogeneously Nucleated Reactions | | | | Homogeneous Reactions |
|---|---|---|---|---|---|
| Thermal Characteristics | Athermal | Thermally Activated | | Growth Controlled By Heat Transport | Thermally Activated |
| Nature of Interface | Glissile (moves under stress alone) | Non-Glissile | | | |
| Degree of Diffusion | None | Short Range (Interface Controlled) | Long Range (Diffusion and/ or Interface Controlled | Either Long or Short Range | Short Range |
| Examples of Transformations | Twinning, Martensite, Stress-Induced Movement of Low Angle Boundaries | Polymorphic Transitions, Growth from Vapor, Recrystallization and Grain Growth, Order-Disorder Changes, Massive-Martensite | Continuous Precipitation, Discontinuous Precipitation, Dissolution, Eutectoid Reactions | Melting, Solidification | Spinodal Some Order-Disorder Changes |

*This table is a simplified version of a more comprehensive classification devised by J. W. Christian.(1)

i.e. short-range diffusion are: polymorphic transitions, recrystallization and grain growth, order-disorder reactions, and massive-martensite reactions; examples involving long-range diffusion are continuous and discontinuous precipitation, and eutectoid reactions. The third type of growth in heterogeneously nucleated solids is the special case in which the growth of the product phase is determined by the rate of heat transfer, i.e., melting or solidification processes.

Homogeneously nucleated solids can be classified in a similar manner. All known homogeneous reactions are thermally activated and the growth of the product phase is limited by short-range diffusional processes. The spinodal is the most familiar type of homogeneously nucleated transformation.

A comparison of martensitic, and nucleation and growth transformations is outlined in Table 3. Athermal and thermally activated growth processes are more familiarly (but less rigorously) known as martensitic, and nucleation and growth (N&G) phase transformations, respectively. This terminology is unfortunate since nucleation and growth processes are common to both types of transformations.

The most distinguishing characteristic of the martensitic transformation is the complete absence of diffusion at the interface of the growing plate. The atomic movements of this transformation are cooperative and thousands of atoms move simultaneously over very small distances, not unlike twinning. The amount of transformation is characteristic of temperature and, with rare exception, does not increase with time. The beginning and end temperatures of the reaction are designated "$M_s$" and "$M_f$", respectively. The $M_s$ and $M_f$ temperatures are primarily determined by composition but are influenced by elastic and plastic deformation and

by grain size.

The martensitic transformation is always accompanied by a change in lattice and in external shape. The shape change, caused by the lattice shear, can be clearly observed on a polished surface in the form of surface tilts and is used as experimental verification of martensitic transformation. A growing martensitic plate is always oriented with respect to the parent phase and the plane common to both is called the "habit" plane. These and other features characteristic of the martensitic transformation are summarized in the left panel of Table 3.

In contrast to diffusionless martensitic transformations, the principal features of N&G transformations reflect the temperature and time dependence of diffusion reactions. In principle, the transformation will continue at any temperature until complete. In practice, at low temperatures relative to the transformation temperature the reaction rate will be negligible due to the low rate of diffusion. The rate of N&G reactions is often accelerated by plastic deformation since both nucleation and diffusion are enhanced. Since the growth rate of the nuclei of new phases is temperature and time dependent, it is possible to "quench-in" high temperature N&G structures by fast cooling. The sigmoidal or "S-shaped" curve of temperature vs time for many N&G reactions is a consequence of the two opposing factors of (a) increasing tendency to form nuclei with decreasing temperature below the transformation temperature and (b) the decreasing growth rate (diffusion rate) of the nucleus with decreasing temperature. Unlike martensitic transformations, the composition of the product is often unlike that of the parent phase. There are examples of N&G transformations, however, wherein the composition of the parent and product phases are identical, viz polymorphic and

order-disorder reactions. These and other characteristics of N&G transformations are summarized in the right panel of Table 3.

The foregoing discussion has suggested, perhaps, that martensitic and N&G transformations occur separately and under widely differing circumstances. This is not always the case. For example, the massive (N&G) and martensitic transformations are very closely related in the Fe-Ni, Fe-Cr, Fe-C, and Fe-N systems.[10] Another example is that of lower bainite, a decomposition product of austenite, which appears to have features of both martensitic and N&G type transformations.[11]

Table 3 A Comparison of the Principal Features of Martensitic, and Nucleation and Growth Phase Transformations

| Martensitic | N and G |
|---|---|
| Possible only in solid state (metallic and non-metallic). No diffusion involved - composition of parent and product the same. | The composition and atomic volume of the products may or may not be related to the original phase. Polymorphic changes in pure metals and order-disorder reactions in alloys are examples of no changes in composition. |
| Amount of transformation is characteristic of temperature, and, with rare exception, does not increase with time. Velocity of transformation usually very high - approaching that of sound waves in solid. Velocity probably is not temperature dependent. Transformation involves a small displacive or shear-like movements of many atoms - each over a very small distance. Start of transformation called "$M_s$"; end called "$M_f$". $M_s$ and $M_f$ in alloys determined primarily by composition. | Amount of transformation increases with time at any temperature until minimum free energy is reached. In principle transformation will continue at any temperature until complete. At a sufficiently low temperature, the rate will be negligible for any N and G transformation. At the transformation temperature, the activation energy for formation of a critical nucleus and the size of the critical nucleus are infinite; therefore, the rate will again be negligible. |
| Both elastic and plastic deformation influence transformation. Highest temperature at which martensite is formed under stress called "$M_D$". $M_s$ can be depressed both by cold-working above $M_s$ and by isothermally holding below $M_s$. Grain size of parent phase influences $M_s$ somewhat. | The rate of N and G reactions is accelerated by plastic deformation since both nucleation and diffusion are enhanced. The sigmoidal or "S-shaped" curve of temperature vs time for many N and G reactions is a consequence of the two opposing factors of (a) increasing tendency to form nuclei with decreasing temperature below the transformation temperature and (b) the decreasing growth rate (diffusion rate) of the nucleus with decreasing temperature. Since the growth rate of nuclei are time and temperature dependent, it is possible to "quench-in" high temperature N and G structures by fast cooling. |

Table 3. (Continued)

| Martensitic | N&G |
| --- | --- |
| Transformation accompanied by both a lattice and a shape change. Surface tilts on a polished surface, caused by lattice shear, are used as experimental verification of a martensitic reaction. Martensitic microstructure usually consists of flat plates that are thin at extremities, i.e., are lenticular in shape. May also be parallelsided bands. Martensite plates are always oriented with respect to the parent phase. Plane on which they are formed is called habit plane. | In solid state N&G reactions strain energy may determine shape of new phase at early reaction times. Crystals of new phase may be oriented to original lattice, i.e., Widmanstatten structure. Often there is no crystallographic relation between parent and product phase. Orientation relationships frequently found when two phases are formed together as in solidification of eutectic alloys or in eutectoidal reactions in solid state. |

## APPENDIX B

### Effect of Strain Energy on Nucleation

Most phase changes are associated with a change in volume. When a small region in a crystal transforms, the rigidity of the surrounding material may be sufficient to allow stresses of considerable magnitude to develop. The volume change associated with the transformation is accommodated in the assembly by elastic strains in the two phases. This elastic strain energy is often an important factor in transformations.

At high temperatures, the flow stresses of the crystals are low and the transformation stresses are relieved by plastic flow, or creep. At low temperatures, the stress will be equal to the flow stress of the material, and the resulting strain energy may be high. Plastic flow can reduce the strain energy, but when the nuclei are small, no dislocations will be present and the stresses may reach values several orders of magnitude greater than the normal yield stress. Furthermore, even if a nucleus formed at or near a Frank-Read dislocation source, the stress field generated by the transformation would not extend far enough to make the dislocations move an appreciable distance, and a single dislocation attached to the surface of a small particle could not relax a spherical stress field. A formulation of the nucleation theory including the strain energy term is presented as Eq. (8).

$$G_{\Delta} = 4/3\pi r^3 \Delta G_v + \pi 4\, r^2 \gamma + 4/3\, r^3 \Delta G_s \qquad (8)$$

where $\Delta G_s$ is the elastic strain energy per unit volume of a spherical nucleus. In the simple treatment the shape of the nucleus was considred to be spherical because this shape requires the minimum surface energy. When strain energy is involved, however, the shape of the nucleus is not necessarily

spherical. There are certain combinations of size and shape which give a minimum value for $\Delta G$. This is so because the strain energy is a function of the shape, as is the surface energy. It is the minimum of the surface energy plus the strain energy that determines what the shape of the nucleus will be. For nuclei of any general shape, the free energy equation may be written as shown in Eq. (9).

$$\Delta G = n\,(g_\beta - g_\alpha + \Delta G_s) + C_1\,\gamma n^{2/3} \tag{9}$$

where $g_\alpha$ and $g_\beta$ are the free energies per atom in the $\alpha$ phase and the $\beta$ phase, respectively, $\Delta G$ is the free energy per atom in the $\beta$ phase, $\Delta G_s$ is the elastic strain energy per atom transformed, $C_1$ is a constant defining the "shape factor", $\gamma$ is the surface energy, and n is the number of atoms in the nucleus.

From Eq. (8) it is evident that nucleation cannot occur at all unless the volume free energy change is greater than the sum of the surface energy and the strain energy terms. The strain energy has been calculated for the case where the particles are spherical. This evaluation is presented as Eq. (10).

$$\Delta g_s = 2\mu_\alpha C_2 \frac{(V_\beta - V_\alpha)^2}{3V_\beta}$$

and

$$C_2 = 3K_\beta/(3K_\beta + 4\mu_\alpha) \tag{10}$$

where $\mu_\alpha$ is the shear modulus of the $\alpha$ phase, $K_\beta$ is the bulk modulus of the $\beta$ phase, and $V_\alpha$ and $V_\beta$ are the specific volumes of the atoms in the $\alpha$ and $\beta$ phases.

When the nucleus is not spherical, a different analysis is involved.

Nabarro[12] proposed a more general solution for precipitated particles with ellipsoidal shapes. He developed an equation for a family of ellipsoids of revolution having semi-axes R, R, and Y. The corresponding strain energy term is given in Eq. (11).

$$g_s = [2\mu_\alpha \frac{(V_\beta - V_\alpha)^2}{3V_\beta}] f(Y/R) \tag{11}$$

where f(Y/R) is a shape factor function. For the case $Y/R = \infty$ the ellipsoid becomes a cylinder and the mathematical model represents needle shaped precipitated particles. For such particles, the strain energy term is given by Eq. (12).

$$\frac{\mu_\alpha}{2} = \frac{(V_\beta - V_\alpha)^2}{V_\beta} \tag{12}$$

In this case, f(Y/R) = 3/4. When Y/R is very much less than 1, the ellipsoidal particles become thin plates or discs. In this case, Nabarro obtained the approximate solution shown in Eq. (13).

$$f(Y/R) \simeq 3\ Y/4R \tag{13}$$

The particle shape that causes the minimum strain energy is a thin flat plate when the conditions of constraint are extreme and when the volume change is appreciable. Although the elastic strain energy term becomes less as the value of f(Y/R) decreases, the surface energy term increases. The most favorable nucleation shape is that which minimizes the total free energy.

The above presentation is by no means complete (see Theory of Transformation, in Metals and alloys by Christian[1]) for a comprehensive treatment of this subject. It is evident, however, that the treatment of nucleation theory

in its formal and complete state is a complicated and difficult problem. It is not difficult to see, therefore, that the correlation between theory and experiment in the case of homogeneous nucleation leaves much to be desired. The problem is further complicated by the fact that homogeneous nucleation is a rarity, except in certain special cases such as the spinodal decomposition of a solid solution. Heterogeneous nucleation is energetically favored when there are defects present in the solid. Such nucleation will be discussed in the next section.

Heterogeneous Nucleation

The preceding discussion was confined to the conditions where the precipitation process was homogeneous throughout the volume of the material. In reality, however, this condition is highly unlikely and rarely occurs. Structural defects such as dislocation networks and grain boundaries are preferential sites for nucleation and it is at these defects that nucleation generally occurs. The reason why heterogeneous nucleation occurs in preference to homogeneous nucleation is that there is a smaller free energy associated with the formation of nuclei at structural defects. Considering first the case where strain energy is not important, the nucleation process then depends upon the reduction in the net surface energy provided by the structural defects to form the nucleus. In the case of dislocation networks and grain boundaries, a reduction in the surface energy requires and involves a destruction of part of an existing surface. Thus the existing surface helps to provide the surface energy needed to form the nucleus.

In considering nucleation at grain boundaries, the surface energy terms involved are $_{\alpha\beta}$ where the first refers to the grain boundary energy and the second to the interfacial energy between the two phases. The free energy in the case of a nucleus forming at a grain boundary is given by Eq. (14), and the criterion for the critical size of thenucleus, or $r_c$,

is given by Eq. (15).

$$\Delta G_{\alpha\beta s} = (C_\beta r^3/V_\beta)(g_\beta - g_\alpha) + r^2 \{C_{\alpha\beta}\ \gamma_{\alpha\beta} + C_{\alpha\alpha}(\gamma_{\alpha\beta} - \gamma_{\alpha\alpha}) \tag{14}$$

For a critical size nucleus, $r_c$, let

$$\frac{\delta \Delta G_{\alpha\beta s}}{\delta r} = 0 \tag{15}$$

Then

$$\Delta G_{\alpha\beta s} = \frac{4}{27} \frac{(C_{\alpha\beta}\ \gamma_{\alpha\beta} - C_{\alpha\alpha}\ \gamma_{\alpha\alpha})^3\ (V_\beta)^2}{(C_\beta)^2 (g_\alpha - g_\beta)^2} \tag{16}$$

where $\Delta G_{\alpha\beta s}$ is the surface free energy for an $\alpha$-$\beta$ interface, $C_\beta$, $C_{\alpha\beta}$, and $C_{\alpha\alpha}$ are shape factor functions, and the other terms are the same as before.

If the surface energy of the $\alpha$-$\beta$ interface is isotropic, the nucleus will be bounded by a section of a spherical surface of radius r. However, the nucleus will not be spherical because other conditions must be met. There must be a balance of surface tension forces where the surface of the nucleus meets the grain boundary. The nucleus will assume a symmetrical lens shape such that $C_{\alpha\beta} = \frac{\pi}{3}(2 - 3\cos\theta + \cos\theta^3)$, $C_{\alpha\beta} = 2\ (1 - \cos\theta)$, $C_{\alpha\alpha} = \sin^2\theta$, and $\theta$ is the correct angle between the $\alpha$-$\beta$ interface and the grain boundary. The condition for static equilibrium is given by Eq.(17).

$$\gamma_{\alpha\alpha} = 2\gamma_{\alpha\beta} \cos\theta \tag{17}$$

The free energy for the formation of a critical nucleus is thus bound to be that given in Eq. (18).

$$\Delta G_{\alpha\beta s} = \frac{8\pi}{3} \frac{(\gamma_{\alpha\beta})^3 (V_\beta)^2 (2-3\cos\theta + \cos^3\theta)}{(g_\alpha - g_\beta)^2} \tag{18}$$

The ratio of the free energy for boundary nucleation to that for homogeneous nucleation is given in Eq. (19), where $\Delta G_B$ indicates the grain boundary free energy and $\Delta G_H$ the free energy for homogeneous nucleation of a precipitated particle.

$$\frac{\Delta G_B}{\Delta G_H} = \frac{1}{2} (2-3 \cos\theta + \cos^3\theta) \tag{19}$$

Nucleation may also occur at the junction with three grains in which case the three planar boundaries meet at a line with the planes, making an angle of 120° to each other. The nucleus spherical surfaces joined at the planar interfaces. Here again, the angle $\theta$ will be used to indicate the dihedral angle between two alpha-beta surfaces and an alpha-alpha surface. Although the geometry is a little more complex in this case, the net result is that the free energy for the formation of a nucleus at an edge $G_{\alpha\beta E}$, formed by the intersection of three grains is given by Eq. (20) and the ratio of the nucleation energy to that for homogeneous nucleation then becomes that shown in Eq. (21).

$$\Delta G_{\alpha\beta E} = 4C_\beta \gamma_{\alpha\beta} V_\beta^2/(g_\beta - g_\alpha)^2 \tag{20}$$

$$\frac{\Delta G_E}{\Delta G_H} = \frac{3C_\beta}{4\pi} \tag{21}$$

$$\text{where } C_\beta = 2\,[\pi - 2\arcsin\left(\tfrac{1}{2}\operatorname{cosec}\theta\right) + (\cos^2\theta)\,\frac{(4\sin^2\theta - 1)^{1/2}}{3} \tag{22}$$

$$- \arccos\left(\cos\theta/\sqrt{3}\right)\cos\theta\,(3-\cos^2\theta)\,]$$

The above analysis was based upon the assumption that the energy gain came entirely from the free energies of the planar boundaries and that the single line at the intersection of the three boundaries did not contribute to the energy of the system.

There is another possible case that should be considered, namely, where four grains intersect at a point. In this case, there are four grain edges which are the junctions of three grains. If it is assumed that these are symmetrically oriented with respect to the corner, then the nucleus will be bounded by spherical surfaces which will have the shape of a spherical tetrahedron. The ratio of the free energy required to form this nucleus ($\Delta G_c$) to that of the homogeneous nucleation is identical in form with Eqs. (21) and (22), except in this case the term $C_\beta$ is given by the expression shown as Eq. (23).

$$C_\beta = [8\,\{\tfrac{\pi}{3} - \arccos\frac{\sqrt{2} - \cos\theta\,(3 - C_{\beta 1}{}^2)^{1/2}}{C_{\beta 1}\sin\theta}\}$$

$$+ (C_{\beta 1}\cos\theta)(4\sin^2\theta - C_{\beta 1}{}^2)^{1/2} - \frac{C_{\beta 1}{}^3}{\sqrt{2}}\cos\theta \tag{23}$$

$$- 4\cos\theta\,(3 - \cos^2\theta)\,(\arccos\frac{C_{\beta 1}}{2\sin\theta})$$

where $C_{\beta 1} = \frac{2}{3}\left[\sqrt{2}\,(4\sin^2\theta - 1)^{1/2} - \cos\theta\right]$.

From Eq. (17) it can be seen that the ratio of the grain boundary energy to the interphase boundary energy is 2 cosθ. When this ratio is used to evaluate the activation energies for homogeneous nucleation, grain boundary nucleation, edge nucleation, and corner nucleation, it becomes evident that $\Delta G_H$ is always greater than $\Delta G_C$, which is always greater than $\Delta G_E$, and that in turn is always greater than $\Delta G_C$. The ratio of the boundary energies becomes zero at some finite value of $\frac{\gamma_{\alpha\alpha}}{\gamma_{\alpha\beta}}$. When the boundary energies are higher, then no equilibrium is possible and the new phase will continue to grow without reaching an equilibrium size. The critical values of the ratios of boundary energies above which the free energy at the critical size is zero, are $2, \sqrt{3}, \frac{2\sqrt{2}}{\sqrt{3}}$ for boundaries, edges, and corners, respectively. Examples of both boundary and edge precipitation are shown in Fig. (10) in the text.

The nucleation rates depend upon the density of sites, as well as upon the activation energy for nucleation. If it is assumed that the thickness of a grain boundary is $T_B$ and that the average grain diameter is $L_B$, then the number of atoms per unit of volume on the various sites can be given by Eq. (24), where $N_B$ is the number of boundaries per unit of volume, $N_E$ is the number of edges per unit volume, and $N_C$ is the number of corners per unit of volume; $N_v$ being the number of atoms per unit of volume

$$\begin{aligned} N_B &= N_v\,(T_B/L_B) \\ N_E &= N_v\,(T_B/L_B)^2 \\ N_C &= N_v\,(T_B/L_B)^3 \end{aligned} \qquad (24)$$

The nucleation rate per unit of volume due to grain boundaries is related to the corresponding homogeneous rate, $I_H$, by Eq. (25).

$$\frac{I_B}{I_H} = \frac{T_B}{L_B} \; \varepsilon^{\frac{\Delta G_B - \Delta G_H}{kT}} \tag{25}$$

Similar equations exist for the nucleation rate along the edges and corners. From these equations it is possible to find the conditions under which the various types of nucleation, i.e. homogeneous, grain boundary, edge, corner, make the greatest contribution to the overall nucleation rate. In principle, if a solid solution is slowly cooled through a phase transformation temperature, nucleation will initially be greatest on corners, then on edges, then on boundaries, and finally, homogeneously. However, since the rates of the reactions vary, if $\gamma_{\alpha\alpha}$ is less than 0.9 $\gamma_{\alpha\beta}$, the corner nucleation rate will be too small to be observed, and edge nucleation will be more rapid than corners. If $\gamma_{\alpha\alpha}$ is less than 0.6 $\gamma_{\alpha\beta}$, the amount of edge nucleation will be small and boundary nucleation will become prevalent. Further, if $\gamma_{\alpha\alpha}$ is less than 0.25 $\gamma_{\alpha\beta}$, only homogeneous nucleation will be observed.

ACKNOWLEDMENT

It is impractical to attempt to credit the numerous contributors to the vast subject of microstructure and phase transformations. Wherever possible, review papers have been suggested for the reader interested in more complete bibliographies.

The authors are indebted to Professor Gareth Thomas of the University of Claifornia for the use of several transmission micrographs of GP zones.

This work was done under the auspices of the United States Atomic Energy Commission.

## References


1. J. W. Christian, "Theory of Transformation in Metals and Alloys", in press.
2. M. Volmer and A. Weber, Phys. Chem. 119 (1925) 277.
3. R. Becker and W. Doring, Ann. Phys. [5] 24 (1935) 719.
4. D. Turnbull and J. Fisher, J. Chem. Phys. 17 (1949) 71.
5. A. Keh and W. Leslie, "Structure and Properties of Engineering Materials", Interscience Publishers, New York, 1963, 108.
6. C. S. Smith, Trans. ASM, 45, (1953) 533.
7. G. Borelius, Trans. AIME (1951) 477.
8. J. W. Cahn, Acta Met., 9 (1961) 795.
9. M. Hillert, Acta Met., 9 (1961) 525.
10. W. S. Owen, "High Strength Materials", John Wiley and Sons, New York, 1965, 167.
11. A. J. Baker, P. M. Kelly, and J. Nutting, "Electron Microscopy and Strength of Crystals", Interscience Publishers, 1962, 899.
12. F. R. N. Nabarro, Proc. Roy. Soc. (London) 52 (1940) 90 and 175, (1940) 519.
13. J. B. Newkirk, "Precipitation from Solid Solution", ASM Monograph, 1959, 77.
14. W. Rostoker and J. R. Dvorak, "Interpretation of Metallographic Structures", Academic Press, 1965, 127.
15. J. B. Newkirk, "Precipitation from Solid Solution", ASM Monograph, 1959, 67.
16. W. S. Owen, "High Strength Materials", John Wiley and Sons, New York, 1965, 404.
17. J. B. Newkirk, "Precipitation from Solid Solution," ASM Monograph, 1959, 79.
18. H. K. Hardy and T. J. Heal, Prog. Met. Phy. 5 (1954) 143.

Fig. 1. A quenched iron - 23.8 at.% nickel alloy with a typical "massive" microstructure (10), X350.

Fig. 2. These micrographs illustrate the variety of shapes that a precipitate from solid solution can assume: (a) General (or matrix) and Local (or grain boundary) precipitation of $\alpha$-iron in copper (13); (b) General and local precipitation in a Ti-6% Cr alloy (14). (The grain boundary precipitate appears as an almost continuous network around the matrix grains; the matrix precipitate is plate-like in nature); (c) Widmanstatten or basket-weave structure in Almoco-2 alloy (15).

Fig. 3. The microstructure of martensite in an Fe-32% Ni alloy, X500 (16). White area showing no structural features is retained austenite.

Fig. 4. Continuous precipitation in a quenched Fe-0.02% Ni alloy aged at several times and temperatures: form left to rignt (1) aged 1 hr at 100°C; (2) 9hrs at 60°C; (3) 68 hrs at 25°C (5).

Fig. 5. Discontinuous and continuous precipitation in an aged Co-Ni-Ti alloy, X2500 (17).

Fig. 6. Variation of free energy, $\Delta G$, with radius of nucleus, r. $\Delta G_s$ is the surface free energy change, $\Delta G_v$ is the volume free energy change, and $\Delta G_N$ is the net free energy change. $\Delta G_c$ is the free energy change associated with the formation of critical nucleus of radius $r_c$.

Fig. 7. Nucleation frequency, I, vs degree of undercooling, $\Delta T$.

Fig. 8. The effect of carbon content on precipitation of carbon from solid solution in 3.3% silicon ferrite, quenched from 775°C.

Fig. 9. Schematic diagram illustrating grain orientation relationships in discontinuous precipitation. The orientation of the

growing α-lamellae is identical to that of grain I but Different from that of grain II. An incoherent interface is thus achieved between the lamellae and grain II.

Fig. 10. An Al-4% Cu alloy, aged 5 hours at 190°C, showing GP zones and θ", X8000. The contrasting halo around each zone is indicative of the strain produced by the zones. The large needle-like precipitates are θ. (Courtesy of G. Thomas, University of California.)

Fig. 11. Hardness-time curve for Al-4% Cu aged at 130°C (after Hardy et al.) (18).

Fig. 12. An Al-4% Cu alloy, aged 20 minutes at 270°C, showing θ' precipitate, X60,000. (Courtesy of G. Thomas, University of California.)

Fig. 13. The Au-Pt phase diagram. The spinodal reaction takes place within the region bounded by the dashed lines.

Fig. 14. Electron micrograph of a thin foil of Cu-20 percent Ni-20 percent Fe alloy showing the "periodic" structure of the precipitate in two grains (18). This periodicity is characteristic of the spinodal reaction.

Fig. 15. Variation of transformation start temperature with cooling rate for pure iron and iron-chromium alloys (10).

Fig. 16. Transformation start temperatures on continuously cooling iron-nickel alloys (10).

ZN-5074

Fig. 1

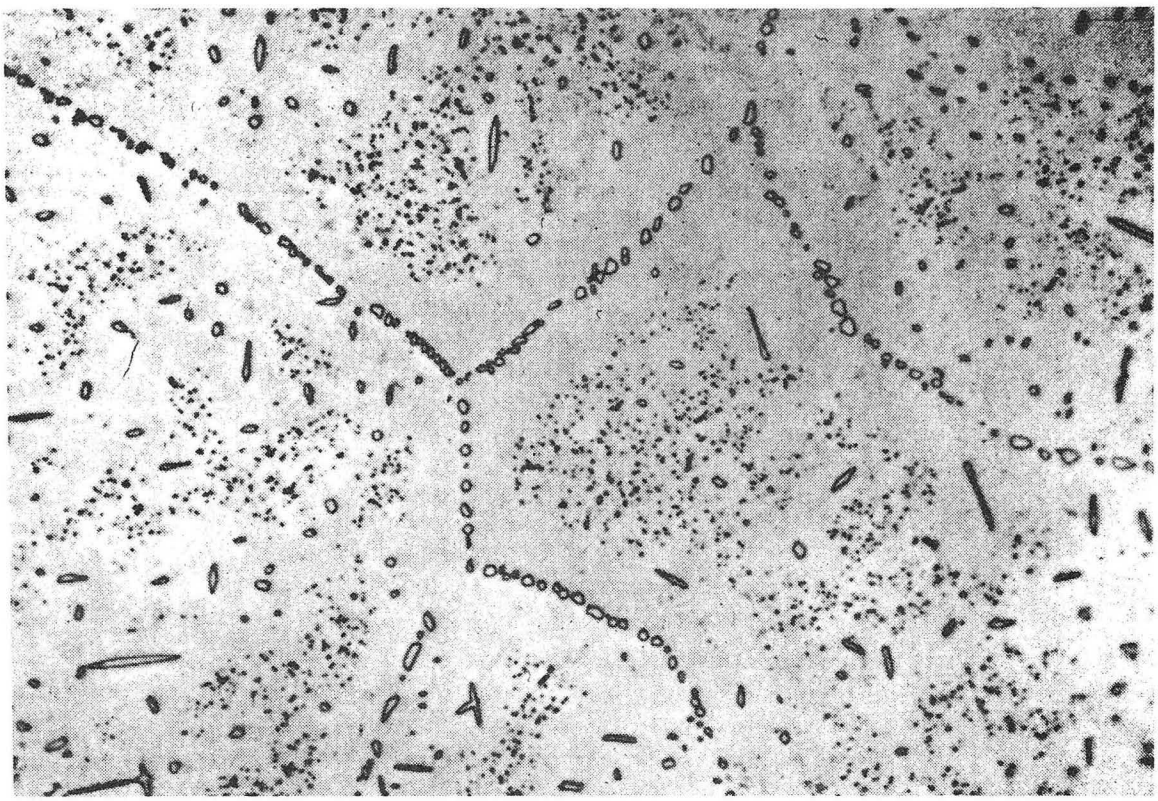

ZN-5069

Fig. 2a

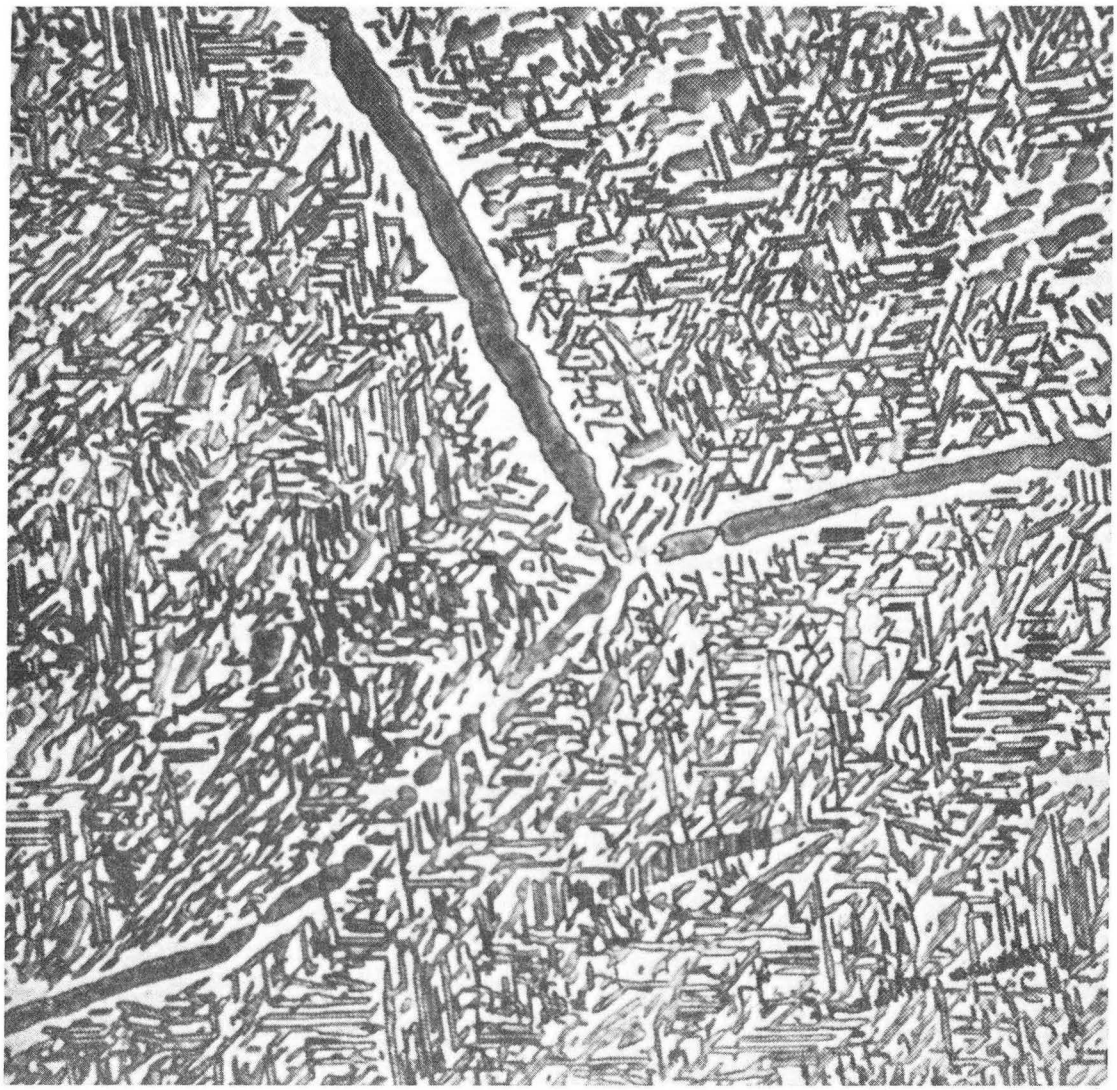

ZN-5759

Fig. 2b

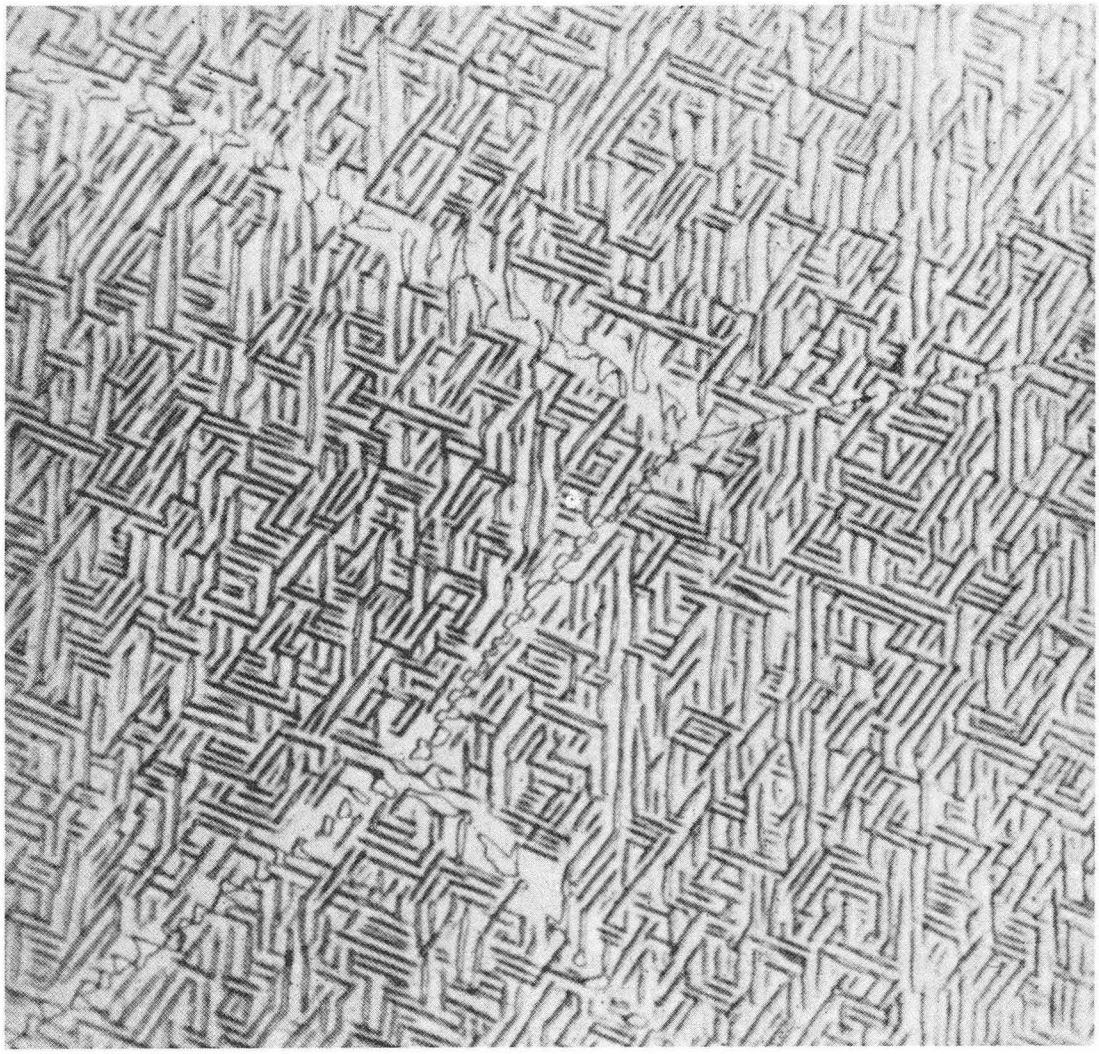

ZN-5760

Fig. 2c

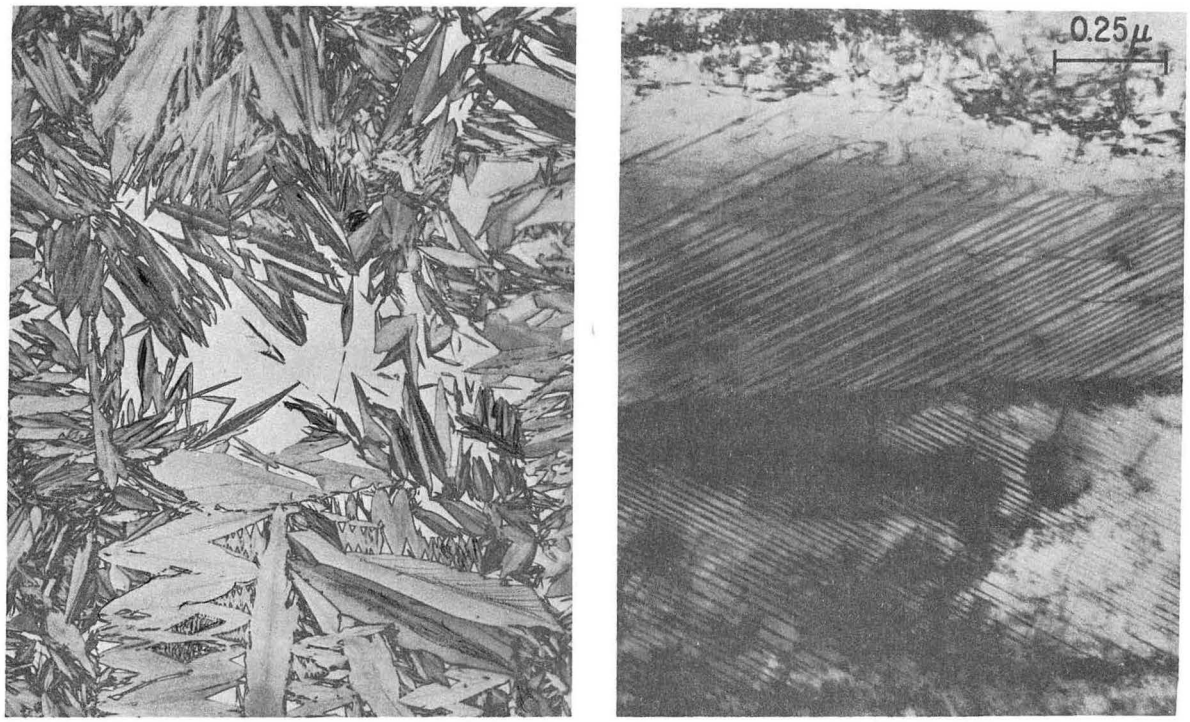


ZN-5070

Fig. 3

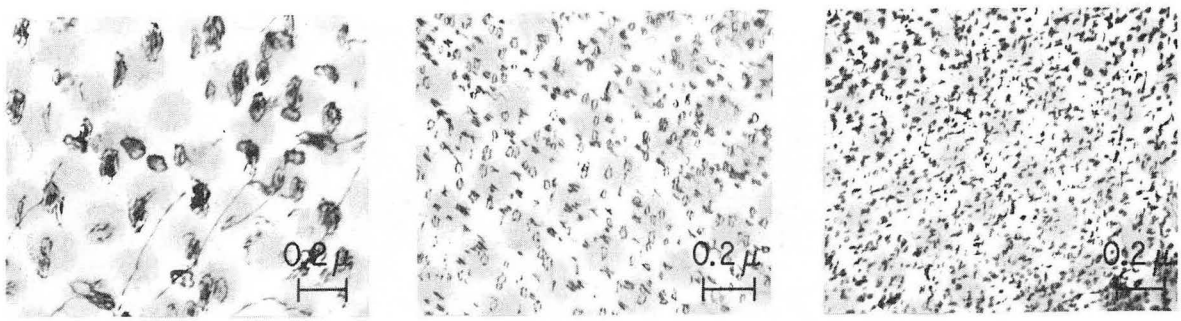


ZN-5073

Fig. 4

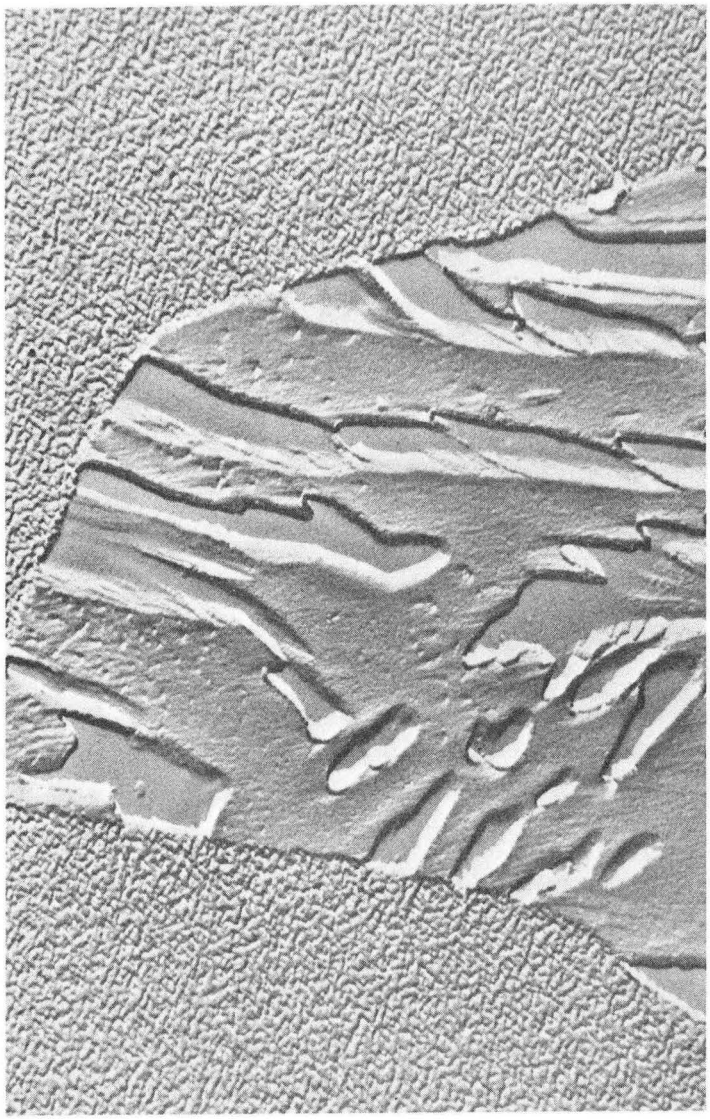

ZN-5727

Fig. 5

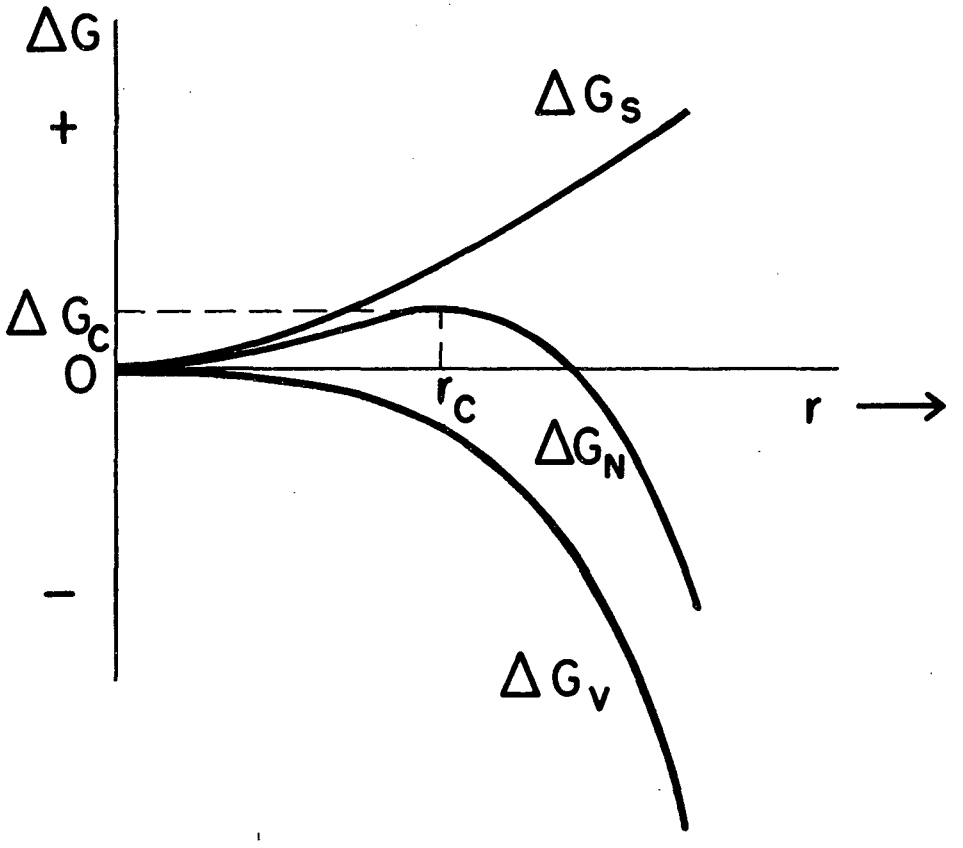


MUB-8057

Fig. 6

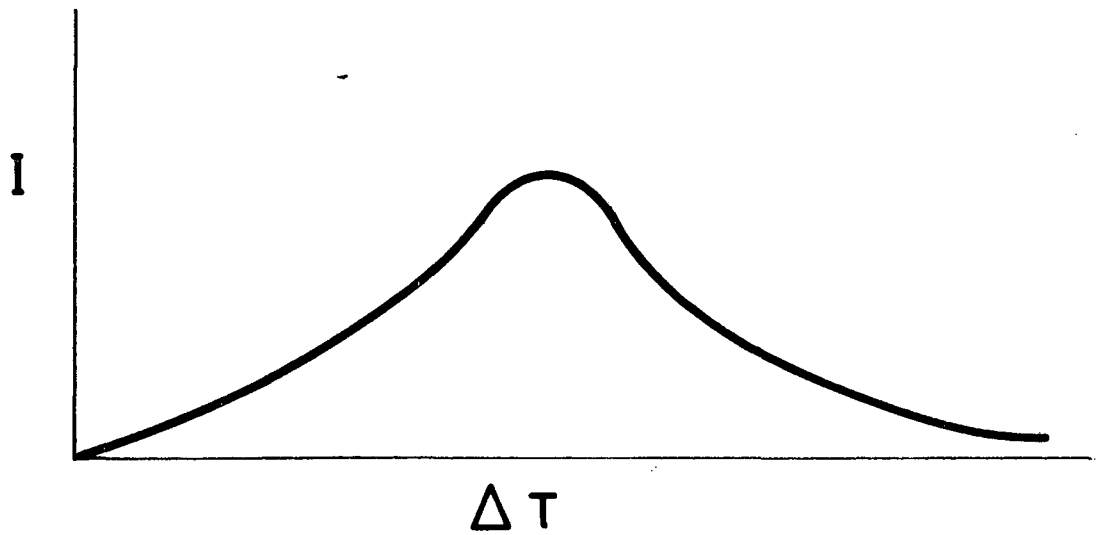


MUB-8056

Fig. 7

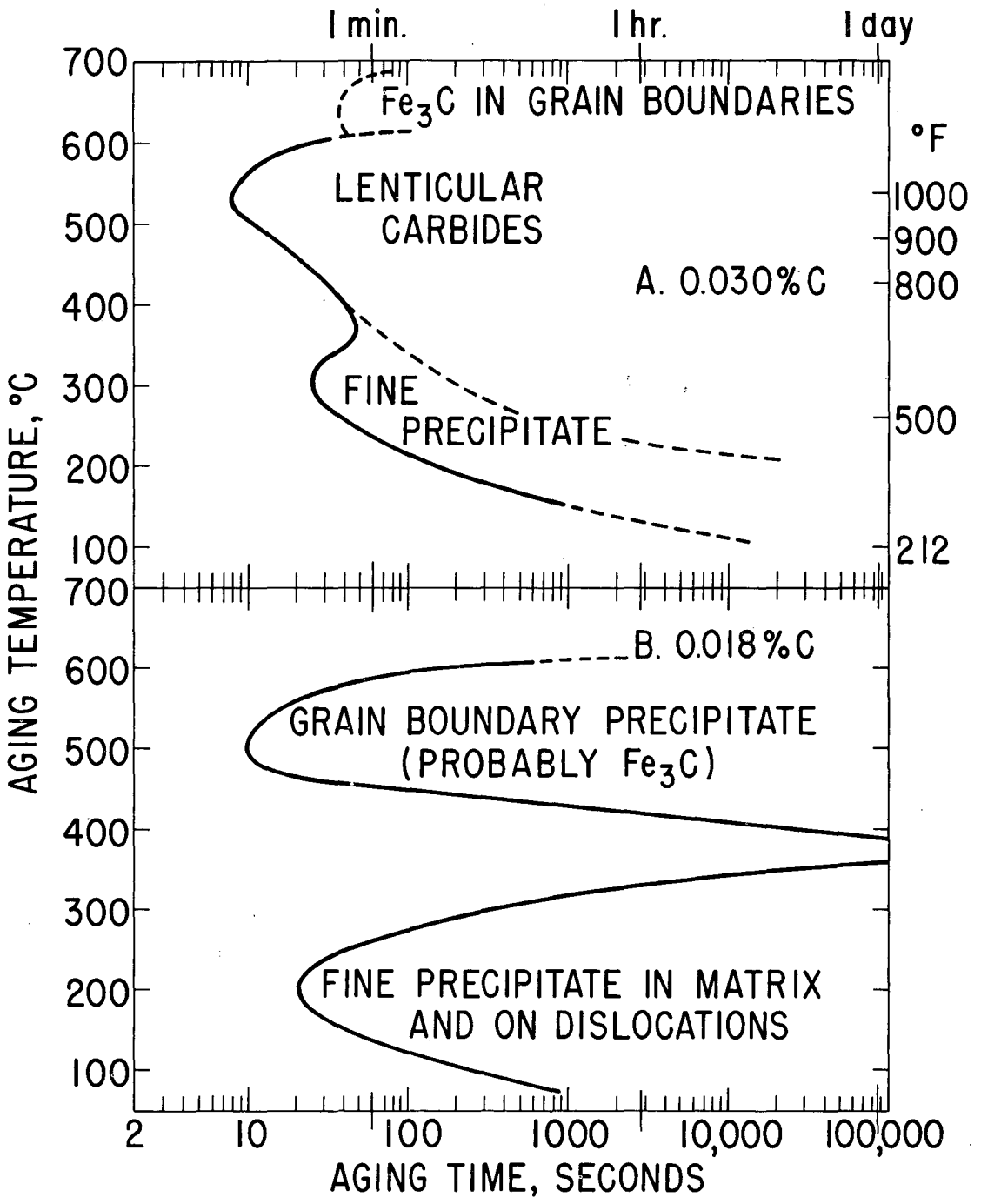


MUB-7390

Fig. 8

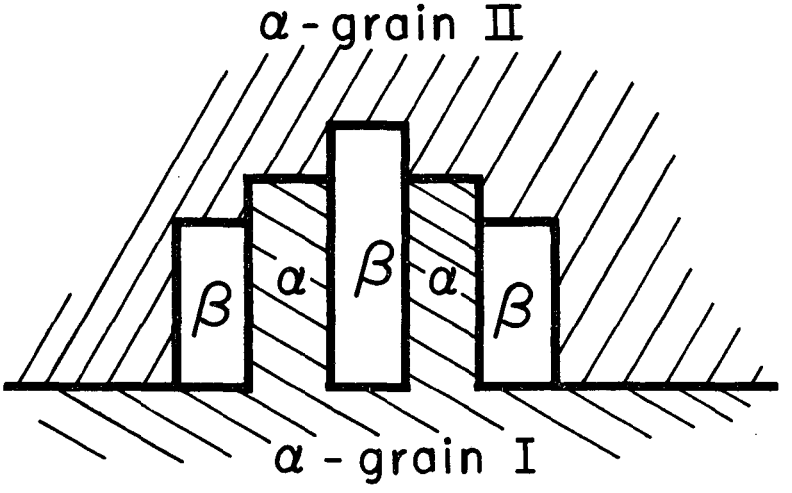


MUB-7281

Fig. 9

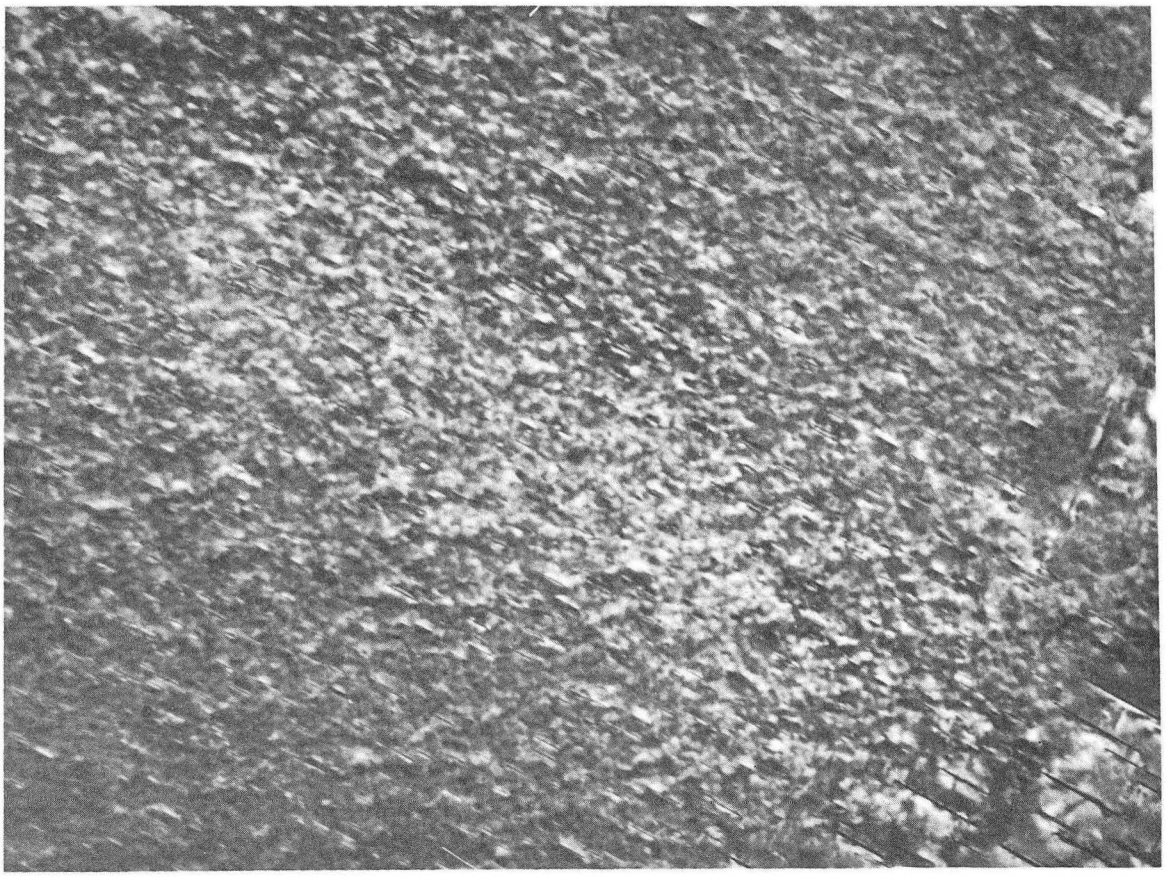

ZN-5071

Fig. 10

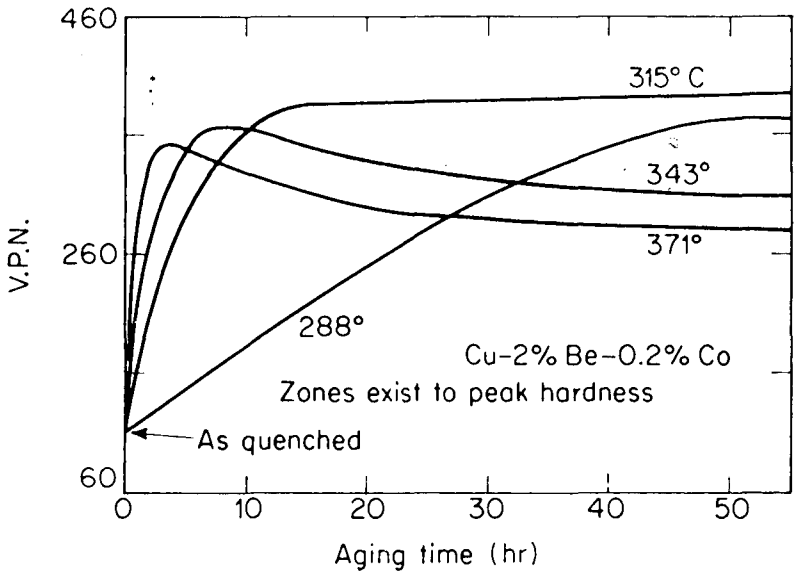


(a)

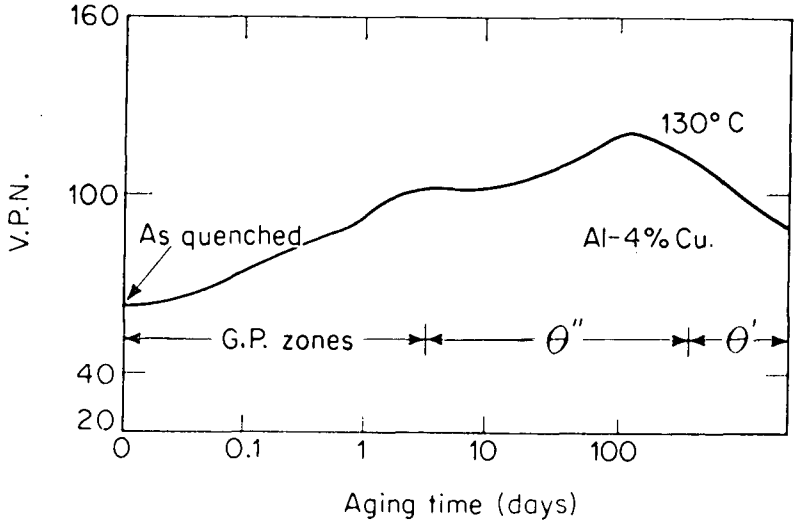


(b)

MUB-7391

Fig. 11

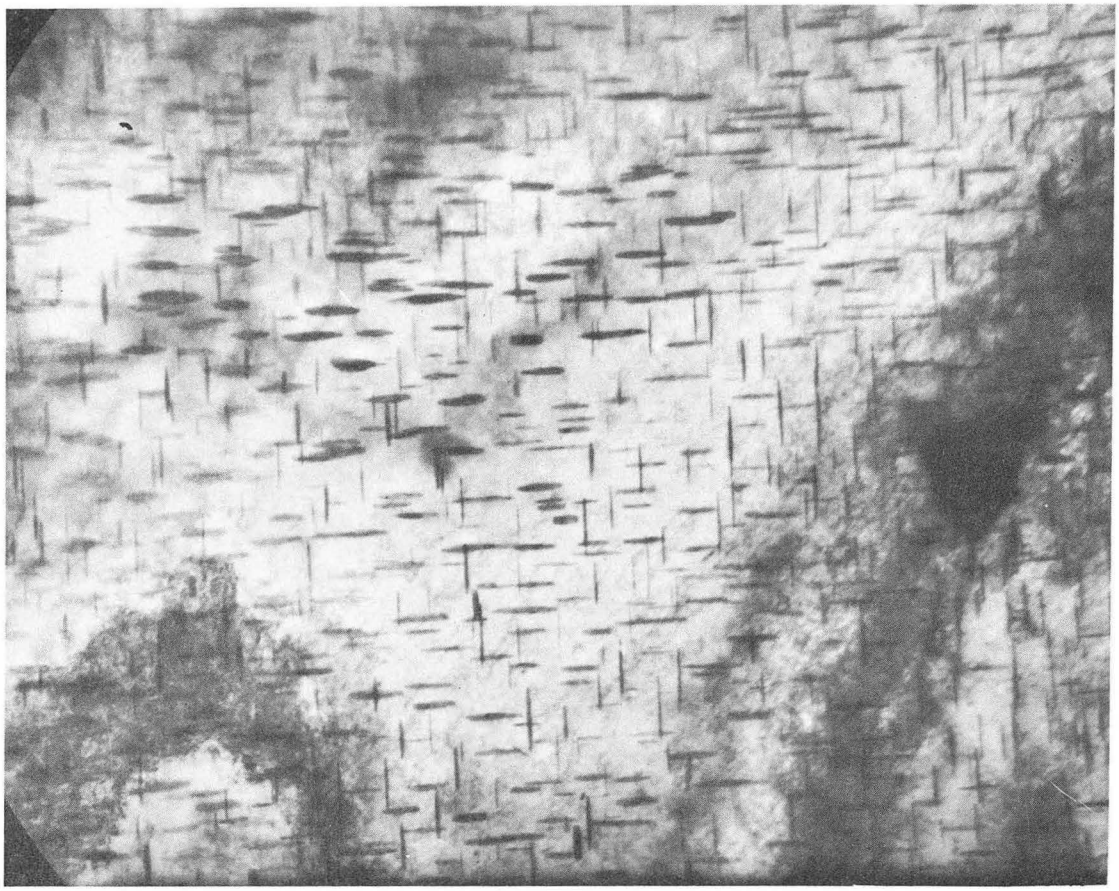

ZN-5072

Fig. 12

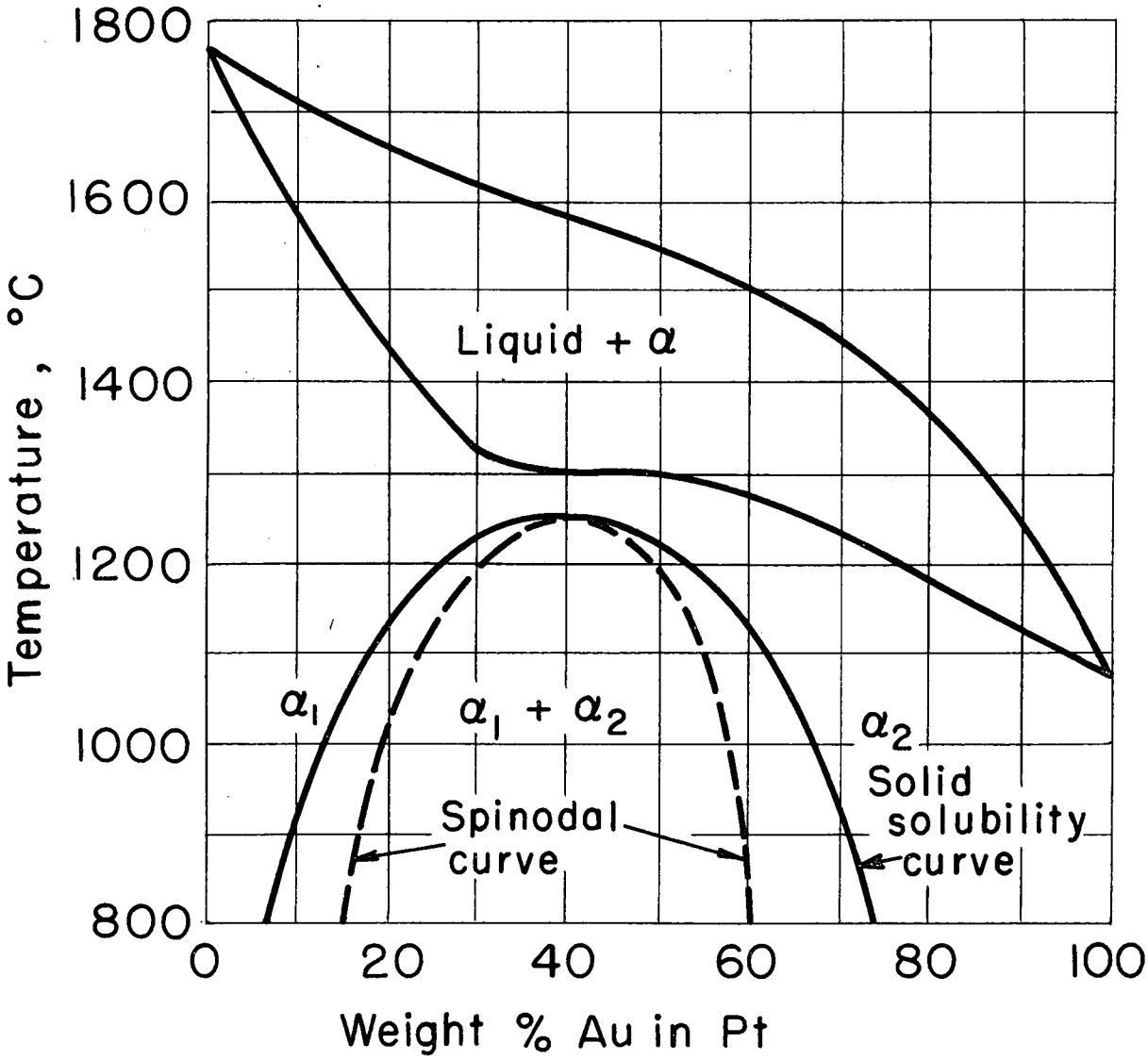


MUB-7282

Fig. 13

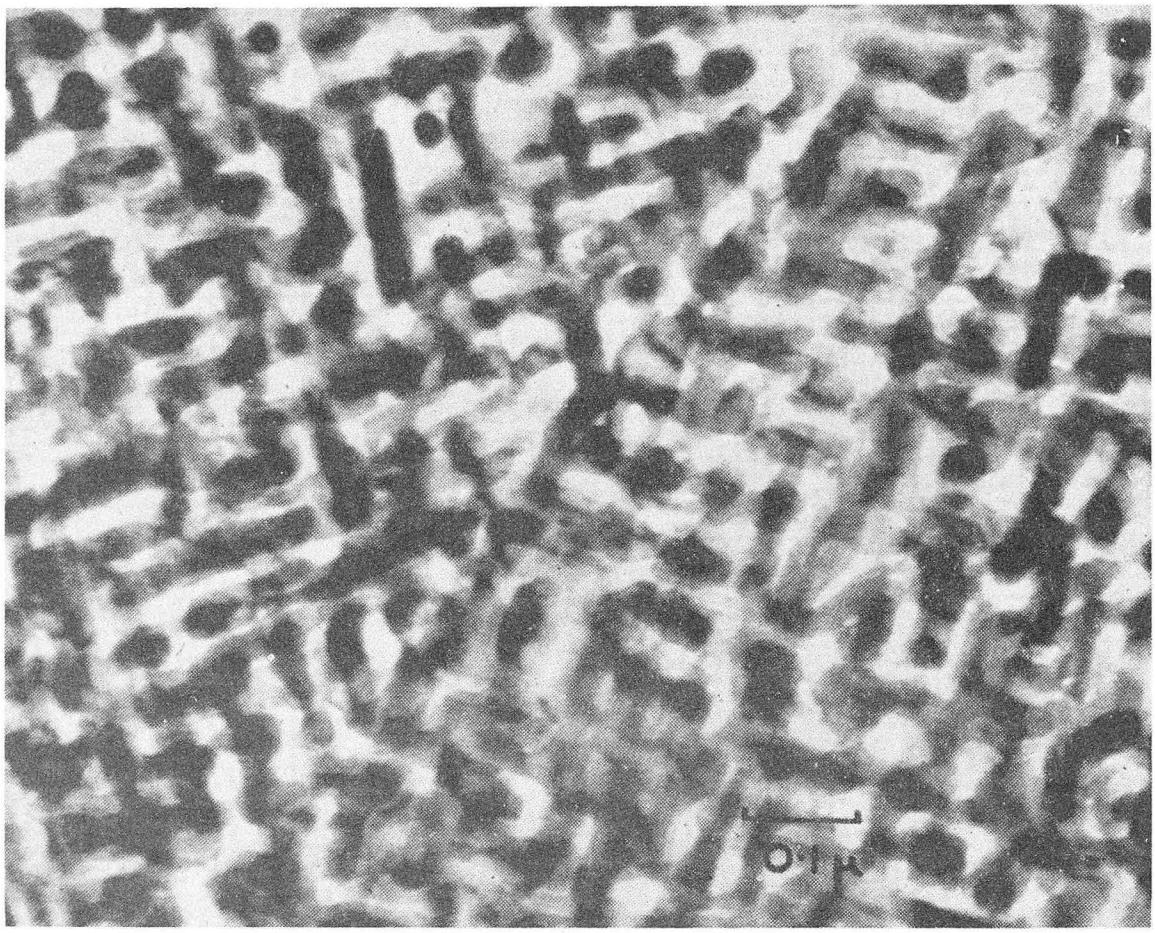


ZN-4436

Fig. 14

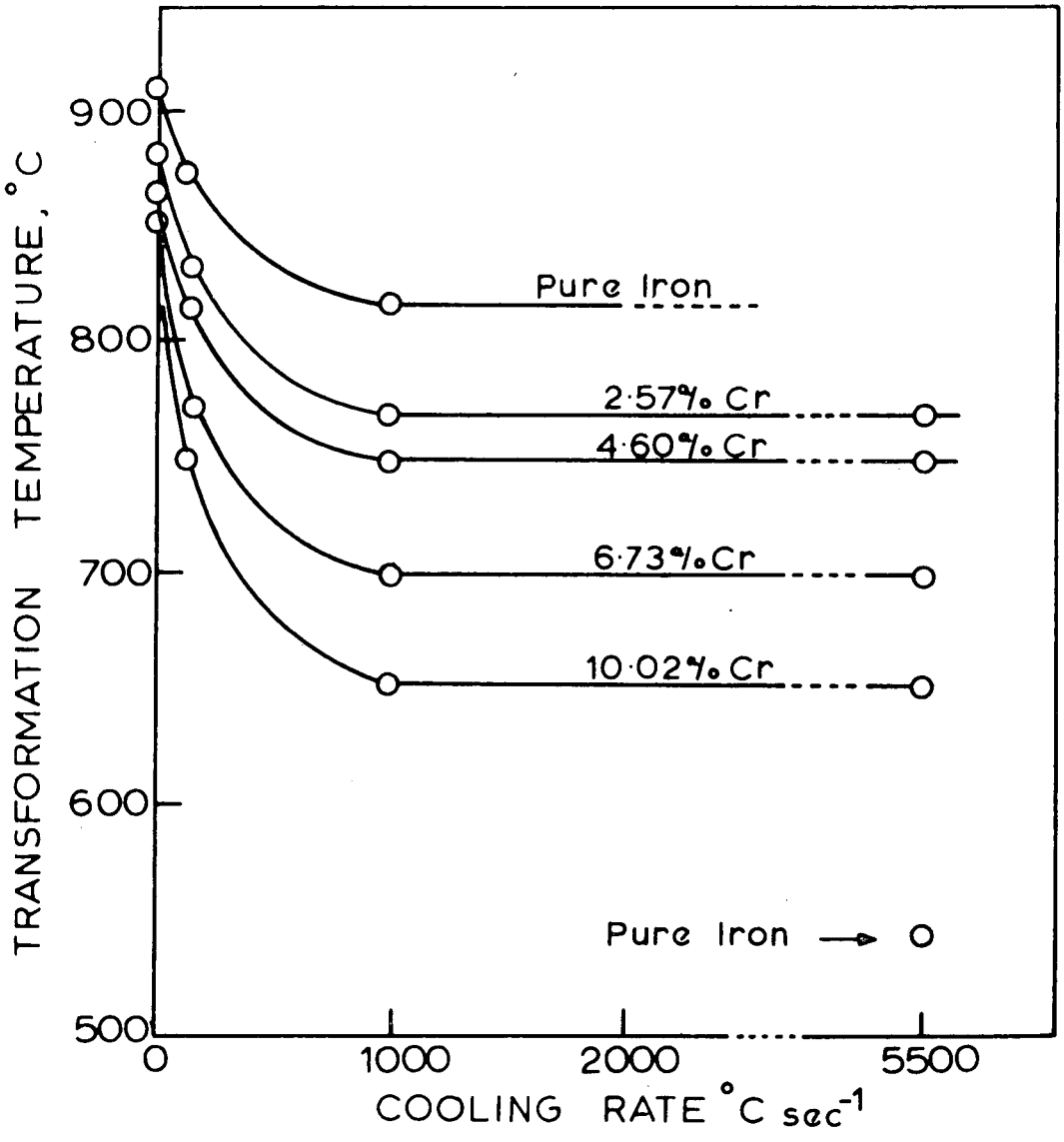


MUB-7389

Fig. 15

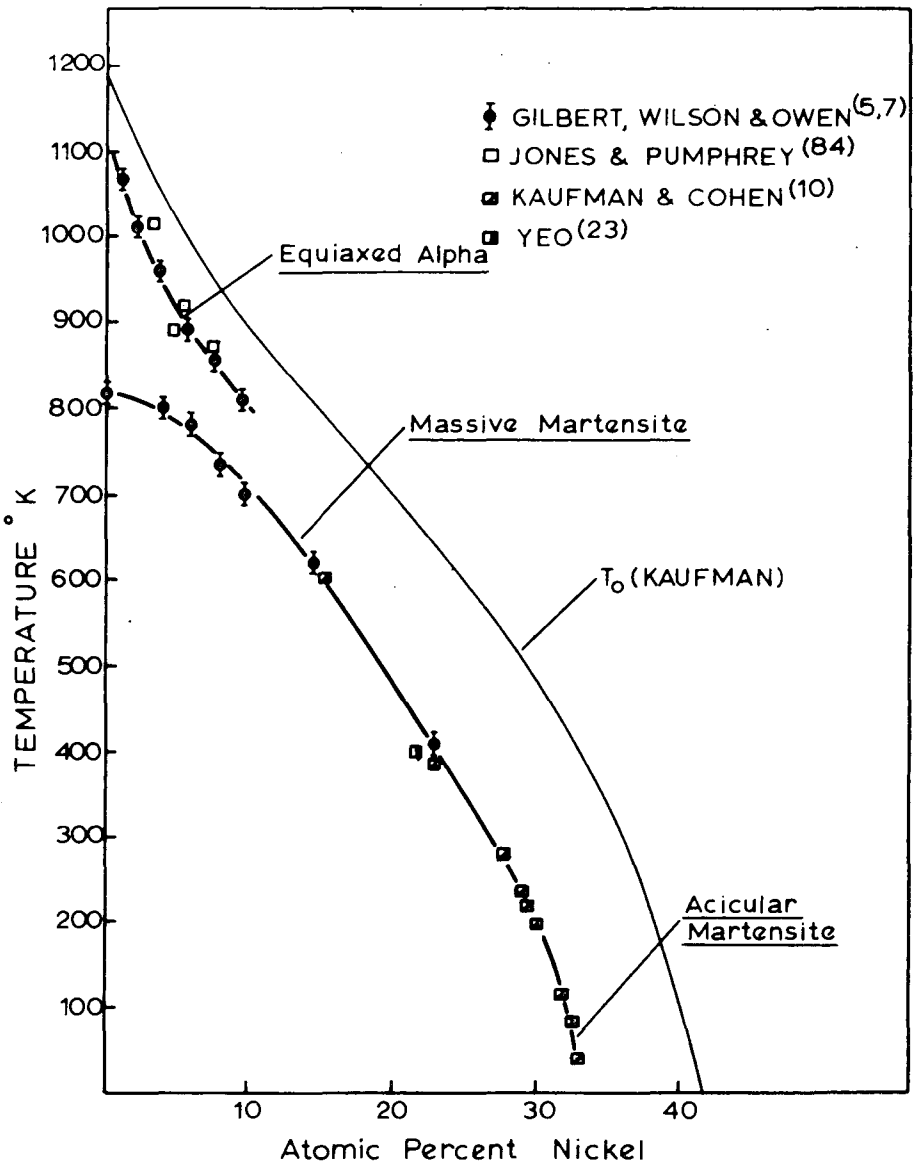


Transformation start temperatures on continuously cooling iron-nickel alloys.

MUB-4349

Fig. 16

This report was prepared as an account of Government sponsored work. Neither the United States, nor the Commission, nor any person acting on behalf of the Commission:

A. Makes any warranty or representation, expressed or implied, with respect to the accuracy, completeness, or usefulness of the information contained in this report, or that the use of any information, apparatus, method, or process disclosed in this report may not infringe privately owned rights; or

B. Assumes any liabilities with respect to the use of, or for damages resulting from the use of any information, apparatus, method, or process disclosed in this report.

As used in the above, "person acting on behalf of the Commission" includes any employee or contractor of the Commission, or employee of such contractor, to the extent that such employee or contractor of the Commission, or employee of such contractor prepares, disseminates, or provides access to, any information pursuant to his employment or contract with the Commission, or his employment with such contractor.